

---

# Variance Reduction in Training Forecasting Models with Subgroup Sampling

---

Yucheng Lu<sup>1,2</sup> Youngsuk Park<sup>2</sup> Lifan Chen<sup>2</sup> Yuyang Wang<sup>2</sup> Christopher De Sa<sup>1</sup> Dean Foster<sup>3</sup>

## Abstract

In real-world applications of large-scale time series, one often encounters the situation where the temporal patterns of time series, while drifting over time, differ from one another in the same dataset. In this paper, we provably show under such heterogeneity, training a forecasting model with commonly used stochastic optimizers (e.g. SGD) potentially suffers large gradient variance, and thus requires long time training. To alleviate this issue, we propose a sampling strategy named *Subgroup Sampling*, which mitigates the large variance via sampling over pre-grouped time series. We further introduce SCott, a variance reduced SGD-style optimizer that co-designs subgroup sampling with the control variate method. In theory, we provide the convergence guarantee of SCott on smooth non-convex objectives. Empirically, we evaluate SCott and other baseline optimizers on both synthetic and real-world time series forecasting problems, and show SCott converges faster with respect to both iterations and wall clock time. Additionally, we show two SCott variants that can speed up Adam and Adagrad without compromising generalization of forecasting models.

## 1. Introduction

Large-scale time series forecasting is prevalent in many real-world applications, such as traffic flow prediction (Vlahogianni et al., 2014), stock price monitoring (Box et al., 2011), weather forecasting (Xu et al., 2019), etc. These applications exclusively involve training a single forecasting model: assuming the future values of interests given the past observations in all the time series follows a static distribution or mapping, a *single* forecasting model is ex-

pected to approximate such distribution or mapping<sup>1</sup> after proper training (Rangapuram et al., 2018; Wang et al., 2019; Salinas et al., 2020).

In practice, however, a time series dataset can be heterogeneous with respect to a single forecasting model (Lee et al., 2018). The heterogeneity here specifically means the underlying distribution may vary across different time series instances due to local effects (Wang et al., 2019; Sen et al., 2019); or is correlated to time, a phenomenon we refer to as *concept drift* (Gama et al., 2014). Despite its vulnerability to heterogeneous dataset, training a single model is inevitable in many cases since deploying multiple models is expensive and sometimes generalizes worse (Montero-Manso & Hyndman, 2020; Oreshkin et al., 2019; Gasthaus et al., 2019).

Aside from heterogeneity, another challenge in modern time series dataset is its large size. For instance, the EC-full dataset from Amazon collects the online sales of 500K different products over 300 days (Seeger et al., 2016). At this scale, stochastic optimizers are usually adopted in training, which refer to a class of optimizers that iteratively modify the model parameters towards an optimum point via repeatedly computing stochastic gradients over some predefined loss functions. In the context of training deep forecasting models, a stochastic gradient generally means back propagation on a minibatch of randomly sampled time series slices (Tealab, 2018). Popular stochastic optimizers include SGD (Bottou, 2010), Adam (Kingma & Ba, 2014), AdaGrad (Ward et al., 2019), etc. These optimizers enjoy low computation costs and are observed to achieve better generalization in many cases (Zhou et al., 2020).

In this paper we point out heterogeneity in time series causes large variance on stochastic optimizers, and can lead to slow training. This happens because, as we will provably show in Section 4, the heterogeneity makes the random sampler suffer from additional noise as training examples are not close in the sense of Euclidean distance on their gradients. To address this, we propose an alternative sampler named *Subgroup Sampling*, which samples over pre-grouped time series. The intuition of subgroup sampling is that the distribution of interests in time series is usually repeating over

---

<sup>1</sup>Department of Computer Science, Cornell University, Ithaca, NY, USA. <sup>2</sup>Amazon Web Services (AWS) AI Labs, Palo Alto, CA, USA. <sup>3</sup>Amazon Research, New York, NY, USA. Correspondence to: Yucheng Lu <y12967@cornell.edu>.

---

<sup>1</sup>In this paper, the term distribution and mapping are used interchangeably.

time horizon or is correlated over instances (Liao, 2005; Aghabozorgi et al., 2015; Maharaj et al., 2019). With proper pre-grouping on the time series examples, the sampler is then able to capture the diversity of the underlying data more efficiently while avoiding sampling similar and redundant gradients repetitively. Furthermore, we propose SCott (Stochastic Subgrouped Control Variate Gradient Descent), an SGD-style optimizer that uses a control variate to utilize subgroup sampling while preserving small computation complexity.

Our contributions can be summarized as follows:

1. We show in theory that even on a simple AutoRegressive (AR) forecasting model, the variance of stochastic optimizers can potentially be arbitrarily large and leads to slow training.
2. We propose subgroup sampling, a sampler working with pre-grouped time series and is able to estimate true gradient with provable smaller variance.
3. We propose SCott, an SGD-style variance reduced optimizer that utilizes the subgroup sampling via control variate. We prove the convergence of SCott on smooth non-convex objectives.
4. We empirically evaluate SCott on both synthetic data and real-world forecasting tasks. We show that SCott is able to speed up SGD, Adam, Adagrad without compromising the generalization of forecasting models.

**Notations.** Throughout this paper, we use  $y_j$  to denote the  $j$ -th coordinate of a vector  $\mathbf{y}$ . We use  $\mathbf{y}_{i,a:b}$  to denote  $[\mathbf{y}_{i,a}, \mathbf{y}_{i,a+1}, \dots, \mathbf{y}_{i,b-1}, \mathbf{y}_{i,b}]$ . For two variables  $g_1$  and  $g_2$ ,  $g_1 = \Omega(g_2)$  means there exists a numerical constant  $c$  such that  $g_1 \geq cg_2$ . We use  $|\mathcal{S}|$  to denote the cardinality of a set  $\mathcal{S}$ . We use  $\mathbb{E}[X]$  and  $\mathbb{V}[X]$  to denote the expectation and variance of a random variable  $X$ , given their existence.

## 2. Related Work

**Parameterized Forecasting Models.** Traditional models such as SSM (Durbin & Koopman, 2012), ARIMA (Zhang, 2003), ETS (De Livera et al., 2011), Gaussian Processes (Brahim-Belhouari & Bermak, 2004) are popular choices for modeling the dynamics of a single time series. Recently, with the rise of deep learning, Deep forecasting models (Faloutsos et al., 2019) have proven particularly well suited at taking advantage of large amounts of data to learn parameters of a single global model over an entire collection of time series (Rangapuram et al., 2018; Wang et al., 2019; Salinas et al., 2020). In such setting, multiple time series are jointly learned.

**Variance Reduction in Model Training.** Variance Reduction is a broad topic in optimization and model training. Several early works (Johnson & Zhang, 2013; Defazio et al., 2014; Nguyen et al., 2017) discuss using control variate

type algorithms to reduce variance on simple problems. They require periodic full gradient computation over the entire dataset. Several algorithms combine mini-batching with control variate to reduce complexity (Li & Li, 2018; Horváth et al., 2020). However, these works are limited to use random sampling. In other works, Cutkosky & Orabona (2019) proposes using momentum to cancel out variance in adjacent optimizer steps. Izmailov et al. (2018) proposes using averaging-type algorithms to mimic model ensemble to reduce variance on the validation set. However, none of these methods are designed specifically for time series, and thus they are not able to capture or utilize the property or metadata of time series datasets.

**Sampling Strategy for Stochastic Optimization.** In the domain of stochastic optimization, random sampler is the folklore sampling techniques used in many stochastic optimizer, e.g. SGD (Zhang, 2004). Additionally, Nagaraj et al. (2019) discusses training using random sampler without replacement. Gao et al. (2015) proposes adopting an active weighted sampler for training. Park & Ryu (2020) discusses sampling with cyclic scanning. In the domain of machine learning fairness, several biased samplers are discussed to ensure the output fairness of model predictions (Iosifidis et al., 2019; Wang et al., 2020; Holstein et al., 2019). The subgroup sampling we discuss in this paper is orthogonal to these prior works.

## 3. Preliminaries

In this section we briefly introduce how a forecasting model is trained via Empirical Risk Minimization framework and have a quick overview of modern stochastic optimizers.

**Problem Statement.** As in other machine learning tasks, training forecasting models is often formulated into the empirical risk minimization (ERM) framework. Given  $N$  different time series:  $\{\mathbf{z}_i\}_{i=1}^N$  where  $\mathbf{z}_{i,t}$  denotes the value of  $i$ -th time series at time  $t$ , let  $\mathbf{x}_{i,t}$  denote the (potentially) available features of  $i$ -th time series at time  $t$ , we aim to train a forecasting model  $F$  with parameters  $\theta$  (Table 1). The training is then formulated by connecting  $F$  with a loss function  $\mathcal{L}$  to be minimized. For instance, given the notation in Table 1, a deterministic model over loss function  $\mathcal{L}$  at prediction time  $t_0$  can be expressed as

$$f_{i,t_0}(\theta) = \mathcal{L}(\mathbf{z}_{i,t_0+1:t_0+\tau_p}, \hat{\mathbf{z}}_{i,t_0+1:t_0+\tau_p}),$$

where  $\hat{\mathbf{z}}_{i,t_0+1:t_0+\tau_p} = F(\mathbf{z}_{i,t_0-\tau_c+1:t_0}, \mathbf{x}_{i,1:T_i}; \theta)$  and  $f_{i,t_0}(\theta) : \mathbb{R}^d \rightarrow \mathbb{R}$  is the loss incurred on the  $i$ -th time series at time  $t_0$ . Popular options for loss functions  $\mathcal{L}$  include Mean Square Error (MSE) Loss, Quantile Loss, Negative Log Likelihood, KL Divergence, etc (Gneiting & Katzfuss, 2014). The training is then formulated as an optimization

Table 1. Quantity of interests to approximate in different forecasting types. Inside the table,  $F$  denotes the model where it takes context and features as input, and then make predictions via model parameters  $\theta$ .  $\tau_c$  and  $\tau_p$  denote the context length and prediction length,  $t_0$  is referred to as prediction time by convention.

| Forecasting Model Type | Mappings/Distributions to Approximate   |
|------------------------|---|
| Deterministic          | $\hat{z}_{it_0+1:t_0+\tau_p} = F(\mathbf{z}_{it_0-\tau_c+1:t_0}, \mathbf{x}_{i_1:T_i}; \theta)$   |
| Probabilistic          | $\hat{\mathbb{P}}(\mathbf{z}_{it_0+1:t_0+\tau_p}   \mathbf{z}_{it_0-\tau_c+1:t_0}, \mathbf{x}_{i_1:T_i}; \theta) = F(\mathbf{z}_{it_0-\tau_c+1:t_0}, \mathbf{x}_{i_1:T_i}; \theta)$ |

problem as

$$\hat{\theta} = \arg \min_{\theta \in \mathbb{R}^d} \left[ f(\theta) = \frac{1}{|\mathcal{D}|} \sum_{i=1}^N \sum_{t=1}^{T_i} f_{i,t}(\theta) \right], \quad (1)$$

where  $T_i$  denotes the maximum prediction time in the  $i$ -th time series. We denote  $\mathcal{D}$  as the set of all the training examples indexed by  $(i, t)$ ,  $\forall 1 \leq i \leq N, \forall 1 \leq t \leq T_i$ . A time series slice with certain length is then used as a single training example<sup>2</sup>.

**Stochastic Gradient Optimizers.** A stochastic gradient optimizer refers to an iterative algorithm that repeatedly updates model parameters with a randomly sampled mini-batch of training examples. Concretely, this stochastic gradient with mini-batch size  $M$  is computed as follows:

$$\nabla f_{\xi}(\theta) = 1/M \sum_{(i,t) \in \xi} \nabla f_{i,t}(\theta), \quad (2)$$

where  $|\xi| = M$  and each element in  $\xi$  is in the form of a tuple  $(i, t)$  where  $i \sim \text{Uniform}[1, N]$  and  $t \sim \text{Uniform}[1, T_i]$ . Popular stochastic optimizers includes SGD, Adam, Adagrad, etc.

## 4. Motivation

Based on the preliminaries, in this section we discuss our motivation from two aspects: (1) Gradient variance can be arbitrarily large and can slow down the training, and (2) Using random sampler on a heterogeneous dataset can induce large variance. Our motivation study is done on the classic AutoRegressive (AR) model<sup>3</sup>.

**Motivation example: AutoRegression with MSE Loss.**

Throughout this section, we consider  $p$ -th order AutoRegressive, or AR( $p$ ) model, which can be expressed as follows:

$$\hat{z}_{i,t} = \epsilon_t + \sum_{j=1}^p \theta_{t-j} z_{i,t-j}, \quad (3)$$

where  $\epsilon_t$  is a Gaussian noise term at time  $t$ . We further consider adopting the Mean Squared Error (MSE) loss function,

<sup>2</sup>In practice, this slice is of length that relates to the context and prediction length as shown in Table 1. A commonly used method to obtain all such segments is to use a sliding window strategy.

<sup>3</sup>Our motivation study certainly does not provide a unified conclusion for arbitrary models, the main purpose of this section is to leverage insights from simple settings.

which is

$$f_{i,t}(\theta) = (\hat{z}_{i,t} - z_{i,t})^2. \quad (4)$$

### 4.1. Large Variance can Slow Down Training

We start from studying the variance of Stochastic Gradient (SG):  $\mathbb{V}[\nabla f_{\xi}(\theta)]$ . For any iterative stochastic gradient optimizer  $\mathcal{A}$ , let  $\theta^{(0)}$  and  $\theta^{(t)}$  denote its initial parameters and its output model parameters after  $t$  iterations respectively. Let  $\xi^{(t)}$  denote the mini-batch sampled in its  $t$ -th iteration. We start from a mild assumption on  $\mathcal{A}$ .

**Assumption 1.** *If stochastic optimizer  $\mathcal{A}$  satisfies  $[\nabla f_{\xi^{(k)}}(\theta^{(k)})]_j = 0$  for every  $t > 0$  and  $k = 1, \dots, t$ , then  $[\theta^{(t)}]_j = [\theta^{(0)}]_j$  holds for any index of parameter  $1 \leq j \leq p$ .*

Assumption 1 is often referred to as "zero-respecting" in optimization theory (Carmon et al., 2019) and widely covers many popular optimizers (e.g. SGD, Adam, Adagrad, RMSProp, Momentum SGD, etc) under arbitrary hyperparameter settings. This states that the SG optimizer  $\mathcal{A}$  will not modify a certain parameter of the model unless a gradient updates it in the training. With Assumption 1, we obtain the following theorem.

**Theorem 1.** *For any AR( $p$ ) model ( $p \geq 1, p \in \mathbb{N}$ ) defined in Equation (3), there exists a time series dataset  $\mathcal{D}$  with  $\max_{i,t} |z_{i,t}| = \delta$ , such that for any stochastic gradient optimizer  $\mathcal{A}$  with any  $\theta^{(0)} \in \mathbb{R}^p$  and hyperparameters, for all  $0 < \epsilon < \frac{\delta^2 p^{-\frac{5}{2}}}{8}$ ,  $\mathcal{A}$  needs to compute at least*

$$T = \Omega \left( \mathbb{V} \left[ \nabla f_{\xi^{(0)}}(\theta^{(0)}) \right] \right) \quad (5)$$

*number of stochastic gradients to find a  $\hat{\theta} \in \mathbb{R}^p$  achieving  $\mathbb{E} \|\nabla f(\hat{\theta})\| \leq \epsilon$ . Furthermore,*

$$\mathbb{V} \left[ \nabla f_{\xi^{(0)}}(\theta^{(0)}) \right] = \Omega(\delta^4 p). \quad (6)$$

Theorem 1 provides important insights in two aspects. Specifically, Equation (5) shows if we wish to find a target model with small error, then the least number of stochastic gradients we need is lower bounded by the complexity of variance on the SG. And this conclusion holds for arbitrary hyperparameter scheduling (even with very small learning rate in gradient descent type optimizers). On the other hand, Equation (6) reveals that the variance of SG can

be arbitrarily large in theory, even with advanced transformation/preprocessing on the dataset such as magnitude scaler<sup>4</sup> (Salinas et al., 2020). As the magnitude of the dataset, or the order of AR model increases, the variance on the SG can increase to infinity in theory.

## 4.2. Heterogeneity Noise with Random Sampling

We proceed to investigate another example to illustrate why time series data can be heterogeneous, and how random sampling could cause extra noise on such dataset. Consider the simplest AR model with  $p = 1$ . Without the loss of generality, we assume the parameter is initialized at point 0:  $\theta^{(0)} = 0 \in \mathbb{R}$ . Now consider a dataset  $\mathcal{D}$  contains a single time series that takes the following form:

$$\underbrace{-1}_{t=1}, -\delta, 1, \delta, \underbrace{-1, -\delta, 1, \delta}_{\text{Temporal Pattern}}, \dots,$$

where  $\delta > 0$  denote some constant. We can see in this example a temporal pattern of length 4 is repeating on the time horizon. With some simple analysis<sup>5</sup>, for all the examples whose prediction time  $t_0$  fulfilling  $t_0 \bmod 2 = 1$ , their global minimas are centering around  $\theta_1^* = \delta$ . We denote all these training examples as  $\mathcal{D}_1$ . Similarly, for all the  $t_0$  with  $t_0 \bmod 2 = 0$ , their global minimas are centering around  $\theta_2^* = -\frac{1}{\delta}$ . We denote all these training examples as  $\mathcal{D}_2$ . In this toy dataset, the heterogeneity comes from the fact that  $\mathcal{D}_1$  and  $\mathcal{D}_2$  are not gathering around the same global minimia: when  $\delta$  increases, the distance of two minimas  $|\delta + 1/\delta|$  centers will increase. We now present the problem with random sampling in the following lemma,

**Lemma 1.** Consider using random sampling on  $\mathcal{D}$  to obtain a mini-batch  $\xi$  with size of  $M = 2$ , then when the training examples in  $\xi$  are either both sampled from  $\mathcal{D}_1$  or both from  $\mathcal{D}_2$ , with high probability,

$$\mathbb{V} \left[ \nabla f_{\xi}(\theta^{(0)}) \right] = \underbrace{O(\delta^2)}_{\text{heterogeneity noise}} + o(\delta). \quad (7)$$

On the otherhand, when the training examples in  $\xi$  are sampled from both  $\mathcal{D}_1$  and  $\mathcal{D}_2$ , with high probability,

$$\mathbb{V} \left[ \nabla f_{\xi}(\theta^{(0)}) \right] = \underbrace{o(\delta)}_{\text{model randomness}}. \quad (8)$$

Lemma 1 shows with random sampling, the variance of the stochastic gradients is closely related to the samples: If the samples are somewhat similar, the variance on the gradient will suffer from an additional term – to which we informally refer as heterogeneity noise.

<sup>4</sup>With proper scaling, the magnitude  $\delta$  can become a limited number, such as 1, making  $\delta^4$  bounded by a constant. However, the lower bound is still proportional to  $p$ , which can be arbitrarily large.

<sup>5</sup>Details are included in the supplementary material.

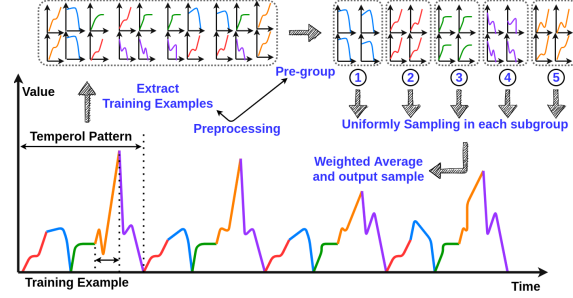


Figure 1. A toy example illustrating subgrouping via temporal pattern. Time series segments placed adjacently with different colors denote different training examples. The same color are pre-grouped by assuming they follow close distribution.

### Algorithm 1 SCott (Stochastic Subgrouped Control Variate Gradient Descent)

**Require:** Total number of iterations  $T$ , learning rate  $\{\alpha_t\}_{1 \leq t \leq T}$ , initialize  $\theta^{(0,0)}$ , The set of groups:  $\{\mathcal{D}_i\}_{1 \leq i \leq B}$ .

1: **for**  $t = 0, 1, \dots, T - 1$  **do**

2: Sample a  $\xi_i^{(t)}$  from subgroup  $i$  and perform subgroup sampling (with  $w_i = |\mathcal{D}_i|/|\mathcal{D}|$ ):

$$\mathbf{g}^{(t,0)} = \sum_{i=1}^B w_i \nabla f_{\xi_i^{(t)}}(\theta^{(t,0)}) \quad (9)$$

3: **for**  $k = 0, 1, \dots, K_t - 1$  **do**

4: Sample  $\xi^{(t,k)}$  from  $\mathcal{D}$ .

5: Compute the update  $\mathbf{v}^{(t,k)}$  as

$$\nabla f_{\xi^{(t,k)}}(\theta^{(t,k)}) - \nabla f_{\xi^{(t,k)}}(\theta^{(t,0)}) + \mathbf{g}^{(t,0)} \quad (10)$$

6: Update the parameters as

$$\theta^{(t,k+1)} = \theta^{(t,k)} - \alpha_t \mathbf{v}^{(t,k)} \quad (11)$$

7: **end for**

8: Set  $\theta^{(t+1,0)} = \theta^{(t,k_t)}$ .

9: **end for**

10: **return** Sample  $\hat{\theta}^{(T)}$  from  $\{\theta^{(t,0)}\}_{t=0}^{T-1}$  with  $\mathbb{P}(\hat{\theta}^{(T)} = \theta^{(t,0)}) \propto \alpha_t B$

## 5. Subgroup Sampling and SCott

In the previous section, we show in Theorem 1 that stochastic optimizers fulfilling Assumption 1 can suffer from large gradient variance, and a random sampler suffers heterogeneity noise from the dataset as shown in Equation (7). In this section, we introduce the design of subgroup sampling and the optimizer SCott, to address these.

### 5.1. Subgroup Sampling over Pre-grouped Time Series

In the toy example shown in Section 4.2: if we always sample from both  $\mathcal{D}_1$  and  $\mathcal{D}_2$ , we are able to reduce the variance as shown in Lemma 1. Here, we discuss how we can extend this idea to a general case.

**Subgroup Sampling Strategy.** Extending our motivation

example in Section 4.2 into a more general case: While we defer the discussion of pre-grouping, suppose the time series dataset is pre-grouped into  $B \in \mathbb{N}^+$  subgroups, i.e.,  $\mathcal{D} = \mathcal{D}_1 \cup \dots \cup \mathcal{D}_B$ , such that each training example  $(i, t)$  (recall Equation (1)) belongs to one unique subgroup. Following the insights from Lemma 1, to eliminate the heterogeneity noise, the target sampler should always guarantee the training examples are sampled from different subgroups. Formally, this sampling strategy can be expressed as

$$\mathbf{g}(\boldsymbol{\theta}) = \sum_{i=1}^B \frac{|\mathcal{D}_i| \nabla f_{\xi_i}(\boldsymbol{\theta})}{|\mathcal{D}|}, \quad (12)$$

where  $\xi_i$  is a set of size  $b$  and each element in  $\xi_i$  is in the form of a tuple  $(j, t)$  where  $(j, t) \sim \text{Uniform}[\mathcal{D}_i]$ . We refer such sampling as *subgroup sampling*. Comparing Equation (12) with (2) we can see the subgroup sampling essentially accumulates the examples from different subgroups and perform a weighted average over them (see Figure 1 for visualization). The property of subgroup sampling is summarized in the following lemma

**Lemma 2.** *Subgroup sampler at any point  $\boldsymbol{\theta} \in \mathbb{R}^d$  satisfies*

$$\mathbb{E}[\mathbf{g}(\boldsymbol{\theta})] = \nabla f(\boldsymbol{\theta}), \quad \mathbb{V}[\mathbf{g}(\boldsymbol{\theta})] = \sum_{i=1}^B \frac{|\mathcal{D}_i|^2 \mathbb{V}[\nabla f_{\xi_i}(\boldsymbol{\theta})]}{|\mathcal{D}|^2}.$$

Lemma 2 reveals subgroup sampling ensures the unbiased estimation of true gradient  $\nabla f$ , and the variance on such sampler *only* depends on the variance of stochastic gradient sampled within each subgroup instead of the entire dataset  $\mathbb{V}[\nabla f_{\xi}(\boldsymbol{\theta})]$ . In other words, subgroup sampling does not suffer additional noise even if the distribution among subgroups are significantly, or even adversarially different.

**Pre-grouping Time Series.** We proceed to discuss how subgroups can be obtained in practice, where the ground truth is not accessible. Precise grouping with arbitrary accuracy is not necessary in practical settings, which may incur substantial computation overhead. As will be shown in the experiments, pre-grouping only based on timestamps (weekdays, seasons), or instance id is sufficient for subgroup sampling to obtain a low-variance output. In the supplementary material we discuss in details on simple pre-grouping algorithms based on the long- and short- term temporal patterns in the dataset (Lai et al., 2018) without extra feature engineering. Despite the sufficiency of a coarse pre-grouping, one can always choose to adopt more advance grouping strategies in practice.

## 5.2. SCott: Stochastic Subgrouped Control Variate Gradient Descent

Despite the mitigation of subgroup sampling on the variance, naively utilizing such sampler in an optimizer is suboptimal since a single sampling requires computation over  $O(B \cdot M)$

Table 2. Difference pre-grouping policy maps SCott to algorithms SCSG (Li & Li, 2018) and SVRG (Johnson & Zhang, 2013) as illustrated in Section 6. Notations are defined in Section 6.

| Pre-grouping Policy | Complexity   | Equivalence |
|---------------------|--|-------------|
| Arbitrary           | Theorem 2  | SCott       |
| Random Hashing      | $O\left(\Delta L \sigma^{\frac{4}{3}} \epsilon^{-\frac{10}{3}}\right)$ | SCSG        |
| Finest-Grained      | $O\left(\Delta L  \mathcal{D} ^{\frac{2}{3}} \epsilon^{-2}\right)$     | SVRG        |

gradients comparing to the  $O(M)$  complexity as shown in Equation (2). To address this, we propose a control variate based design on top of subgroup sampling. Our intuition is that by periodically performing a subgroup sampling and computing some snapshot gradients over the training trajectory, we can use those gradients as estimation anchors to reduce variance while allowing the optimizers to adopt flexible mini-batch sizes in the effective iterations. In other words, we seek to achieve an intermediate solution between the plain subgroup sampling and stochastic optimizers, so that we can benefit from both worlds.

The formal description of such algorithm, which we refer to as SCott, is shown in Algorithm 1. Note that SCott has separate outer and inner iteration loops. A subgroup sampling is only performed in each outer loop in Equation (9) and the output of subgroup sampling  $\mathbf{g}^{(0,t)}$  is then used as control variate<sup>6</sup> in inner loop as in Equation (10).

## 6. Convergence Analysis

In this section, we derive the convergence rate of SCott. We first start from several assumptions.

**Assumption 2.** *The loss on all the single training example  $f_{i,t}, \forall i, t$  is  $L$ -smooth: for some constant  $L > 0$ ,*

$$\|\nabla f_{i,t}(\boldsymbol{\theta}_1) - \nabla f_{i,t}(\boldsymbol{\theta}_2)\| \leq L \|\boldsymbol{\theta}_1 - \boldsymbol{\theta}_2\|, \forall \boldsymbol{\theta}_1, \boldsymbol{\theta}_2 \in \mathbb{R}^d.$$

Assumption 2 is a standard assumption in optimization theory. Note that smooth function is not necessarily convex, which implies our theory works with non-convex models, e.g. deep neural networks with sigmoid activations. We also make the assumption on the sampling variance as follows.

**Assumption 3.** *For all  $\boldsymbol{\theta} \in \mathbb{R}^d$ ,  $i = 1, \dots, B$  and  $t = 0, \dots, T - 1$  in Equation (9), there exists a constant  $\sigma_i^2$  s.t.*

$$\mathbb{V}_{\xi_i \sim \mathcal{D}_i}[\nabla f_{\xi_i}(\boldsymbol{\theta})] \leq \sigma_i^2.$$

The constant  $\sigma_i^2$  in Assumption 3 denotes the upper bound on the gradient variance when random sampling is performed inside the  $i$ -th subgroup. For the convenience of later discussion, we further denote  $\sigma^2$  as the upper bound on

<sup>6</sup>Refer to (Nelson, 1990) for principles on the control variate.

the variance when random sampling over the entire dataset:  $\mathbb{V}_{\xi \sim \mathcal{D}}[\nabla f_{\xi}(\boldsymbol{\theta})] \leq \sigma^2$ . Without the loss of generality, we let  $M = 1$  in our theory. Based on the two assumptions, the convergence rate of Algorithm 1 is shown in the following theorem

**Theorem 2.** Denote  $\Delta = f(\mathbf{0}) - \inf_{\boldsymbol{\theta}} f(\boldsymbol{\theta})$  and  $w_i = |\mathcal{D}_i|/|\mathcal{D}|$ . For any  $\epsilon > 0$ , if we pre-group the dataset  $\mathcal{D}$  into  $\{\mathcal{D}_i\}_{i=1}^B$  such that  $\sum_{i=1}^B w_i^2 \sigma_i^2 = O(\epsilon^2)$ , and let inner loop iterations  $K_t \sim \text{Geo}(B/(B+1))^7$ , Algorithm 1 needs to compute at most

$$T = O\left(\frac{\Delta L \left(B \sum_{i=1}^B w_i^2 \sigma_i^2\right)^{\frac{2}{3}}}{\epsilon^{\frac{10}{3}}} + \frac{\Delta L |\mathcal{D}|^{\frac{2}{3}} \mathbb{I}\{B = |\mathcal{D}|\}}{\epsilon^2}\right)$$

number of stochastic gradients to ensure  $\mathbb{E} \left\| \nabla f \left( \hat{\boldsymbol{\theta}}^{(T)} \right) \right\| \leq \epsilon$ .

If we deliberately let all the subgroup maintain the same size, the convergence rate can be simplified as follows.

**Corollary 1.** Following Theorem 2, if all the subgroups are the same size, i.e.,  $|\mathcal{D}_i| = |\mathcal{D}_j| > 1, \forall i, j$ , Algorithm 1 needs to compute at most

$$T = O\left(\frac{\Delta L \left(B^{-1} \sum_{i=1}^B \sigma_i^2\right)^{\frac{2}{3}}}{\epsilon^{\frac{10}{3}}}\right) \quad (13)$$

number of stochastic gradients to ensure output  $\hat{\boldsymbol{\theta}}^{(T)}$  fulfills  $\mathbb{E} \left\| \nabla f \left( \hat{\boldsymbol{\theta}}^{(T)} \right) \right\| \leq \epsilon$ .

**Remark 1: Consistent with Other Algorithms.** Theorem 2 demonstrates SCott can be seen as a general form of other control variate type algorithms. Specifically, when we group the examples by random hashing, i.e., cyclically assign each example into  $B$  subgroups, then the executions of SCott matches with SCSG (Li & Li, 2018). On the other hand, if we adopt finest-grained grouping, i.e.,  $B = |\mathcal{D}|$ , then executions of SCott is aligned with SVRG (Johnson & Zhang, 2013).

**Remark 2: Reduced Variance Dependency.** Note that  $\sum_{i=1}^B w_i^2 \sigma_i^2 = O(\epsilon^2)$  can always be fulfilled since we can at least select  $B = |\mathcal{D}|$  where  $\sigma_i^2 = 0$ , as in that case every subgroup only contains one sample. If this precondition is somehow violated, it may only guarantee suboptimality in theory, converging to a noisy ball with  $\sum_{i=1}^B w_i^2 \sigma_i^2$ . However, comparing to other stochastic control variate type optimizers, including (Li & Li, 2018) and (Babanezhad et al., 2015), where noise ball is in the order of  $O(\sigma^2)$ , SCott is able to reduce the dependency only on the inner subgroup variance, i.e., from  $\sigma^2$  to  $B \sum_{i=1}^B w_i^2 \sigma_i^2$  (and  $B^{-1} \sum_{i=1}^B \sigma_i^2$

<sup>7</sup>Geo( $p$ ) is the geometric distribution with  $p$ , i.e.,  $\mathbb{P}(K_t = K) = p^K(1-p), \forall K = 0, 1, \dots$

with Corollary 1). In other words, SCott does not compromise the benefit of subgroup sampling shown in Lemma 2.

**Remark 3: Understanding the Selection of  $K_t$ .** The number of inner loops per outer loop ( $K_t$ ), i.e., the frequency of performing a subgroup sampling is a crucial design choice. Theorem 2 show that a Geometric distributed selection helps with the convergence, which is a technique used in other analysis of control variate type algorithms (Li & Li, 2018; Horváth et al., 2020). In practice, we can optimize such selection via an additional hyperparameter: in the supplementary material, we discuss using  $\|\mathbf{v}^{(t,k)}\|^2 \leq \gamma \|\mathbf{v}^{(t,0)}\|^2$  as an additional criterion to terminate the inner loop for some hyperparameter  $\gamma$ .

**Remark 4: Improved Complexity Compared to Stochastic Optimizers.** Carmon et al. (2019) shows the theoretical lower bound on the complexity of stochastic optimizers is  $\Omega(\Delta L \sigma^2 \epsilon^{-4})$ , Comparing Corollary 1 with this bound, we can observe a complexity improvement of at least  $O(\epsilon^{-\frac{2}{3}})$  from SCott compared to stochastic optimizers. On the other hand, as also shown in Table 2, the convergence rate of SCott improves upon SCSG and stochastic optimizers in the sense that its upper bound depends only on the inner subgroup sampling variance.

## 7. Experiment

In this section we empirically evaluate our algorithms and investigate how SCott improves optimizers in practice. We implement SCott in PytorchTS, a time series forecasting library (Rasul et al., 2020). All the tasks run on a local machine configured with a 2.6GHz Inter (R) Xeon(R) CPU and a NVIDIA GTX 1080 GPU.

In Section 7.1 and Section 7.2, we focus on comparing SCott with SGD and SCSG in different settings. These optimizers all have SGD-type update formula, which helps us better understand the effect of variance reduction. Additionally, in Section 7.3, we modify the main step of SCott and let it follow the update rule of Adam and Adagrad. We rerun the experiments from previous sections on the two SCott variants.

**Models and Loss functions.** In this section, we focus on four representative settings in forecasting problems:

- (deterministic) Vector AutoRegressive Model (VAR) with MSE loss (Lai et al., 2018).
- (deterministic) LSTM with MSE loss (Maharaj et al., 2019). We set the hidden layer size to be 100 and the depth to be 2.
- (probabilistic) Simple FeedForward Network (MLP) with Negative Log Likelihood (NLL) loss (Alexandrov et al., 2019). We set the hidden layer size to be 80 and the depth to be 4.
- (probabilistic) N-BEATS with MAPE loss (Oreshkin

Table 3. Performance with different algorithms **given the same time budget for training**. We compute the loss over the entire training and test dataset in the last 10 iterations and present their average. All the optimizers are fine tuned in each task. The **bold** number is the one that has smallest loss.

| Setting: Model/Loss/Time budget  | Optimizer | Exchange Rate |              | Traffic      |              | Electricity |             |
|--|-----------|---------------|--------------|--------------|--------------|-------------|-------------|
|  |           | Train Loss    | Test Loss    | Train Loss   | Test Loss    | Train Loss  | Test Loss   |
| FeedForward Network (MLP)<br>Negative Log Likelihood Loss<br>Time budget: 0.5 hour | SGD       | -1.82         | -1.72        | -2.38        | -2.44        | 6.51        | 5.55        |
|  | SCSG      | -2.03         | <b>-1.73</b> | -2.61        | -2.67        | 6.42        | 5.47        |
|  | SCott     | <b>-2.12</b>  | -1.68        | <b>-2.86</b> | <b>-2.81</b> | <b>6.30</b> | <b>5.34</b> |
|  | Adam      | -2.76         | -2.94        | -2.59        | -2.59        | 6.38        | 5.48        |
|  | S-Adam    | <b>-3.91</b>  | <b>-3.03</b> | <b>-3.03</b> | <b>-3.02</b> | <b>5.73</b> | <b>5.01</b> |
|  | Adagrad   | -3.48         | -3.21        | -2.69        | -2.76        | 6.18        | 5.29        |
|  | S-Adagrad | <b>-3.88</b>  | <b>-3.23</b> | <b>-2.86</b> | <b>-2.89</b> | <b>6.02</b> | <b>5.18</b> |
| N-BEATS<br>MAPE Loss<br>Time budget: 3 hours                                       | SGD       | 1.23          | 1.34         | 2.79         | 3.02         | 0.62        | 0.67        |
|  | SCSG      | <b>1.03</b>   | <b>1.18</b>  | 2.02         | 2.64         | 0.61        | 0.63        |
|  | SCott     | 1.07          | 1.22         | <b>1.89</b>  | <b>2.37</b>  | <b>0.51</b> | <b>0.54</b> |
|  | Adam      | 0.69          | 0.77         | 1.01         | 1.03         | 0.58        | 0.69        |
|  | S-Adam    | <b>0.51</b>   | <b>0.59</b>  | <b>0.80</b>  | <b>0.81</b>  | <b>0.44</b> | <b>0.52</b> |
|  | Adagrad   | 0.76          | 0.80         | 2.06         | 1.99         | 0.53        | 0.63        |
|  | S-Adagrad | <b>0.56</b>   | <b>0.69</b>  | <b>1.48</b>  | <b>1.72</b>  | <b>0.42</b> | <b>0.51</b> |

et al., 2019). We set the number of stacks to be 30.

### 7.1. Warm-up: Synthetic Dataset

We start from training VAR and LSTM on a synthetic dataset, where we know the ground-truth for subgroups. We generate the synthetic dataset by repeatedly transforming a linear curve based on simple functions such as *sin* and *polynomial*. For brevity, the details for generating the dataset is discussed in the supplementary material. We plot the results of SGD and SCott from Figure 2(a) to 2(d). We show SGD and SCott with the fine-tuned learning rate while for SGD we show the top three curves with different learning rate. In Figure 2(a) and Figure 2(c). For SGD, if the learning rate is large, then the convergence curve contains a lot of noise and thus leads to noisy convergence. To ensure stable convergence, SGD needs to adopt small learning rate, and that results in more iterations to converge. SCSG, on the other hand, slightly improve over SGD, while is still noisy in later iterations. By comparison, SCott contains less variance noise, and it allows us to use larger learning rate while keeping a stable convergence.

### 7.2. Real World Applications

We proceed to discuss the performance on real-world applications. In this experiment, we train the FeedForward Network and N-BEATS. We use three public benchmark datasets: *Traffic*, *Exchange-Rate* and *Electricity* (Lai et al., 2018), where details can be found in the supplementary material.

**Pre-grouping Strategy.** We adopt a simple timestamp-based pre-grouping for all the datasets. For *Traffic* dataset:

we group all the time series slices only based on its weekday and season, i.e., two time series slices are in the same subgroup if and only if their weekday and season are the same. This results in total 49 subgroups, we repeat this process on *Electricity* dataset and it results in 70 subgroups; For *Exchange-Rate* dataset, we first evenly divide the whole time series into 6 range based on the time stamps. And then within each range we further group the time series slices based on the time series instance, this results in total 32 subgroups.

**Results.** We first see from Table 3 that given same time budget, SCott achieves smaller loss on both training and testset. We further plot the training curves in Figure 2(e) to 2(f) and Figure 4(a) to 4(b). We can observe the results are mostly aligned with our results on synthetic dataset: with subgroup sampling, SCott is able to adopt large learning rate which allows it to converge faster compared to SGD and SCSG. Additionally, we verify in Figure 2(g) and 4(c) the benefits of SCott does not compromise the validation error of the model. Finally, we plot in Figure 2(h) and 4(d) that the subgroup sampling does induce smaller variance compared to random sampling, even with the simple pre-grouping policy we adopt.

### 7.3. Variants of SCott

So far, we focus on comparing SCott with SGD and SCSG. Moreover, we investigate how SCott can be applicable to enhance other types of optimizers, Adam and Adagrad. To do so, we incorporate the main step of SCott in Equation (11) into the update rule of Adam and Adagrad, which we refer to as S-Adam and S-Adagrad. We rerun all the experiments on the real-world dataset. We first see from Table 3 S-Adam/S-

## Variance Reduction in Training Forecasting Models with Subgroup Sampling

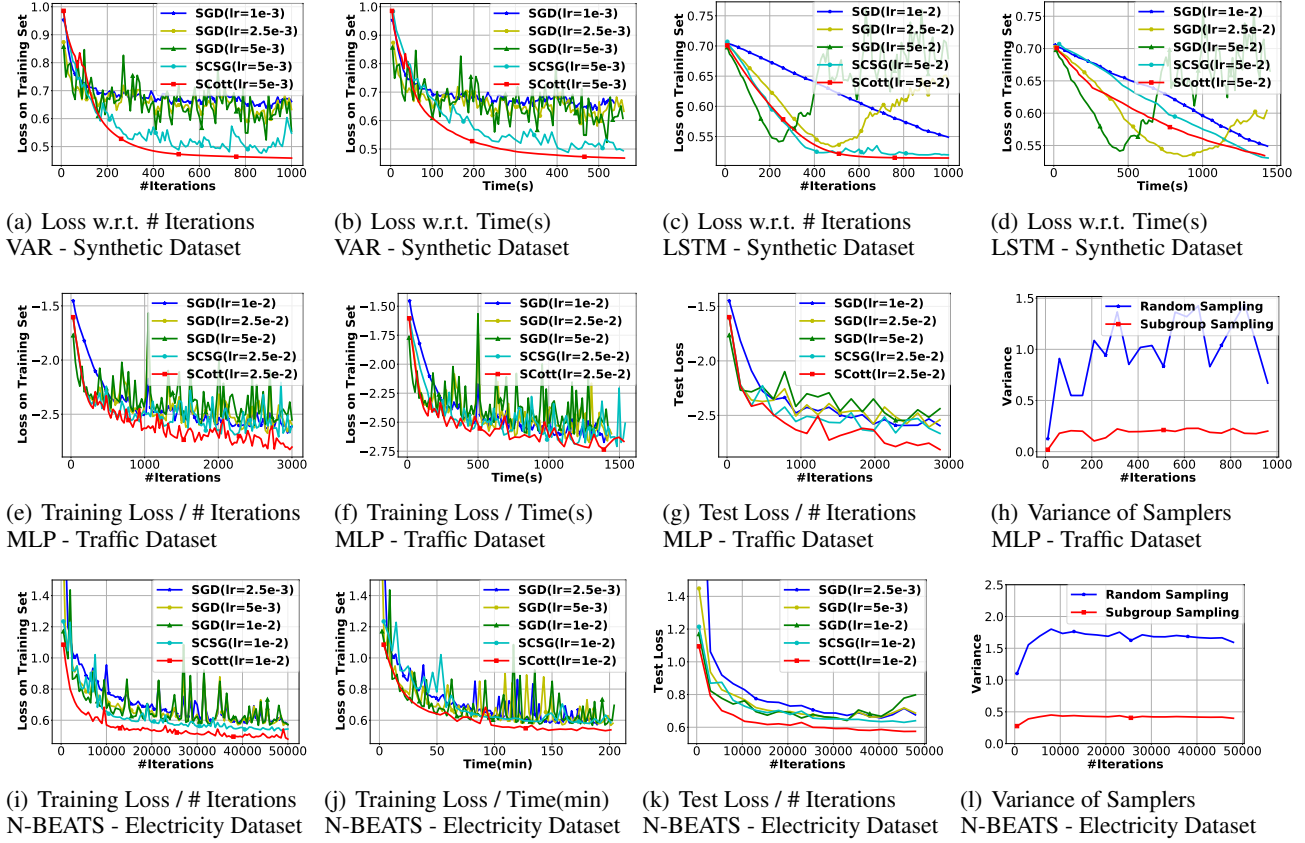


Figure 2. Performance of different optimizers. This experiment focus on comparing SCott with original SGD-type algorithms.

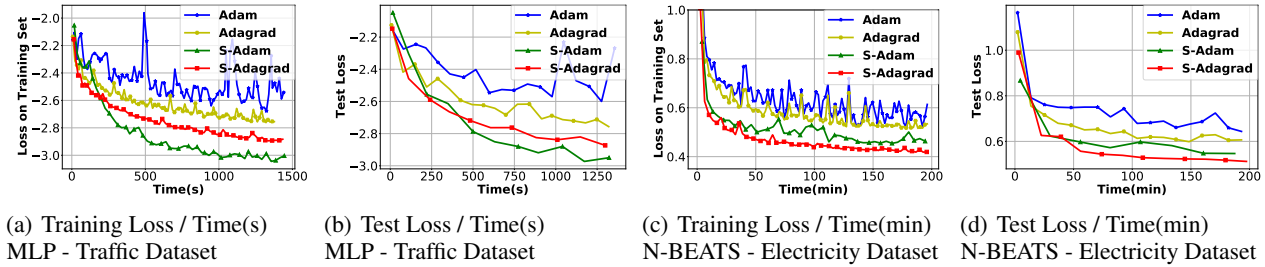


Figure 3. SCott Variants on Adam and Adagrad. The "S-" denotes SCott version of the optimizer. The results are fine tuned.

Adagrad is able to achieve smaller loss given same time. Then we further plot the training curves in Figure 3. We find SCott is able to improve both Adam and Adagrad by a certain margin. As shown in Table 3, these SCott variants improve upon their non-SCott baselines without compromising the test loss. Additionally, comparing SGD-type with Adam- and Adagrad-type optimizers, SCott sometimes can outperform Adam and Adagrad (such as in MLP on traffic dataset). On the other hand, we find S-Adam and S-Adagrad consistently outperform SGD-type optimizers as well as Adam and Adagrad.

## 8. Conclusions

In this paper, we show that heterogeneity in large scale time series data is detrimental to the convergence of the

stochastic optimizers. To address the challenge, we introduce SCott, a variance reduced optimizer that speeds up the training of forecasting models based on pre-grouped time series data. A novel convergence analysis is provided for SCott, which by varying the grouping conditions, recovers the well-known results in stochastic optimization. Empirically, we show SCott converges faster compared to plain stochastic optimizer, with respect to both iterations and time on both synthetic and real-world dataset. We leave the future works of investigating the effect of subgrouping on SCott variants, applying SCott tasks beyond forecasting, and developing practical stepsize selection (Park et al., 2020; Yu et al., 2020).



## References

- Aghabozorgi, S., Shirkhorshidi, A. S., and Wah, T. Y. Time-series clustering—a decade review. *Information Systems*, 53:16–38, 2015.
- Alexandrov, A., Benidis, K., Bohlke-Schneider, M., Flunkert, V., Gasthaus, J., Januschowski, T., Maddix, D. C., Rangapuram, S., Salinas, D., Schulz, J., et al. Gluon-ts: Probabilistic time series models in python. *arXiv preprint arXiv:1906.05264*, 2019.
- Babanezhad, R., Ahmed, M. O., Virani, A., Schmidt, M., Konečný, J., and Sallinen, S. Stop wasting my gradients: Practical svrg. *arXiv preprint arXiv:1511.01942*, 2015.
- Babanezhad Harikandeh, R., Ahmed, M. O., Virani, A., Schmidt, M., Konečný, J., and Sallinen, S. Stopwasting my gradients: Practical svrg. *Advances in Neural Information Processing Systems*, 28:2251–2259, 2015.
- Bottou, L. Large-scale machine learning with stochastic gradient descent. In *Proceedings of COMPSTAT’2010*, pp. 177–186. Springer, 2010.
- Box, G. E., Jenkins, G. M., and Reinsel, G. C. *Time series analysis: forecasting and control*, volume 734. John Wiley & Sons, 2011.
- Brahim-Belhouari, S. and Bermak, A. Gaussian process for nonstationary time series prediction. *Computational Statistics & Data Analysis*, 47(4):705–712, 2004.
- Carmon, Y., Duchi, J. C., Hinder, O., and Sidford, A. Lower bounds for finding stationary points i. *Mathematical Programming*, pp. 1–50, 2019.
- Cutkosky, A. and Orabona, F. Momentum-based variance reduction in non-convex sgd. In *Advances in Neural Information Processing Systems*, pp. 15236–15245, 2019.
- De Livera, A. M., Hyndman, R. J., and Snyder, R. D. Forecasting time series with complex seasonal patterns using exponential smoothing. *Journal of the American statistical association*, 106(496):1513–1527, 2011.
- Defazio, A. and Bottou, L. On the ineffectiveness of variance reduced optimization for deep learning. *arXiv preprint arXiv:1812.04529*, 2018.
- Defazio, A., Bach, F., and Lacoste-Julien, S. Saga: A fast incremental gradient method with support for non-strongly convex composite objectives. *Advances in neural information processing systems*, 27:1646–1654, 2014.
- Durbin, J. and Koopman, S. J. *Time series analysis by state space methods*. Oxford university press, 2012.
- Faloutsos, C., Flunkert, V., Gasthaus, J., Januschowski, T., and Wang, Y. Forecasting big time series: Theory and practice. In *Proceedings of the 25th ACM SIGKDD International Conference on Knowledge Discovery & Data Mining*, pp. 3209–3210, 2019.
- Gama, J., Žliobaitė, I., Bifet, A., Pechenizkiy, M., and Bouchachia, A. A survey on concept drift adaptation. *ACM computing surveys (CSUR)*, 46(4):1–37, 2014.
- Gao, J., Jagadish, H., and Ooi, B. C. Active sampler: Lightweight accelerator for complex data analytics at scale. *arXiv preprint arXiv:1512.03880*, 2015.
- Gasthaus, J., Benidis, K., Wang, Y., Rangapuram, S. S., Salinas, D., Flunkert, V., and Januschowski, T. Probabilistic forecasting with spline quantile function rnns. In *The 22nd International Conference on Artificial Intelligence and Statistics*, pp. 1901–1910, 2019.
- Gneiting, T. and Katzfuss, M. Probabilistic forecasting. *Annual Review of Statistics and Its Application*, 1:125–151, 2014.
- Holstein, K., Wortman Vaughan, J., Daumé III, H., Dudik, M., and Wallach, H. Improving fairness in machine learning systems: What do industry practitioners need? In *Proceedings of the 2019 CHI conference on human factors in computing systems*, pp. 1–16, 2019.
- Horváth, S., Lei, L., Richtárik, P., and Jordan, M. I. Adaptivity of stochastic gradient methods for nonconvex optimization. *arXiv preprint arXiv:2002.05359*, 2020.
- Iosifidis, V., Fetahu, B., and Ntoutsi, E. Fae: A fairness-aware ensemble framework. In *2019 IEEE International Conference on Big Data (Big Data)*, pp. 1375–1380. IEEE, 2019.
- Izmailov, P., Podoprikin, D., Garipov, T., Vetrov, D., and Wilson, A. G. Averaging weights leads to wider optima and better generalization. *arXiv preprint arXiv:1803.05407*, 2018.
- Johnson, R. and Zhang, T. Accelerating stochastic gradient descent using predictive variance reduction. *Advances in neural information processing systems*, 26:315–323, 2013.
- Kingma, D. P. and Ba, J. Adam: A method for stochastic optimization. *arXiv preprint arXiv:1412.6980*, 2014.
- Lai, G., Chang, W.-C., Yang, Y., and Liu, H. Modeling long- and short-term temporal patterns with deep neural networks. In *The 41st International ACM SIGIR Conference on Research & Development in Information Retrieval*, pp. 95–104, 2018.

- Lee, R., Kochenderfer, M. J., Mengshoel, O. J., and Silberman, J. Interpretable categorization of heterogeneous time series data. In *Proceedings of the 2018 SIAM International Conference on Data Mining*, pp. 216–224. SIAM, 2018.
- Lei, L., Ju, C., Chen, J., and Jordan, M. I. Non-convex finite-sum optimization via scsg methods. In *Advances in Neural Information Processing Systems*, pp. 2348–2358, 2017.
- Li, Z. and Li, J. A simple proximal stochastic gradient method for nonsmooth nonconvex optimization. In *Advances in neural information processing systems*, pp. 5564–5574, 2018.
- Liao, T. W. Clustering of time series data—a survey. *Pattern recognition*, 38(11):1857–1874, 2005.
- Maharaj, E. A., D’Urso, P., and Caiado, J. *Time series clustering and classification*. CRC Press, 2019.
- Montero-Manso, P. and Hyndman, R. J. Principles and algorithms for forecasting groups of time series: Locality and globality. *arXiv preprint arXiv:2008.00444*, 2020.
- Nagaraj, D., Jain, P., and Netrapalli, P. Sgd without replacement: Sharper rates for general smooth convex functions. In *International Conference on Machine Learning*, pp. 4703–4711. PMLR, 2019.
- Nelson, B. L. Control variate remedies. *Operations Research*, 38(6):974–992, 1990.
- Nguyen, L. M., Liu, J., Scheinberg, K., and Takáč, M. Sarah: A novel method for machine learning problems using stochastic recursive gradient. *arXiv preprint arXiv:1703.00102*, 2017.
- Oreshkin, B. N., Carpov, D., Chapados, N., and Bengio, Y. N-beats: Neural basis expansion analysis for interpretable time series forecasting. *arXiv preprint arXiv:1905.10437*, 2019.
- Park, Y. and Ryu, E. K. Linear convergence of cyclic saga. *Optimization Letters*, 14(6):1583–1598, 2020.
- Park, Y., Dhar, S., Boyd, S., and Shah, M. Variable metric proximal gradient method with diagonal barzilai-borwein stepsize. In *ICASSP 2020-2020 IEEE International Conference on Acoustics, Speech and Signal Processing (ICASSP)*, pp. 3597–3601. IEEE, 2020.
- Rangapuram, S. S., Seeger, M. W., Gasthaus, J., Stella, L., Wang, Y., and Januschowski, T. Deep state space models for time series forecasting. In *Advances in neural information processing systems*, pp. 7785–7794, 2018.
- Rasul, K., Sheikh, A.-S., Schuster, I., Bergmann, U., and Vollgraf, R. Multi-variate probabilistic time series forecasting via conditioned normalizing flows. *arXiv preprint arXiv:2002.06103*, 2020.
- Salinas, D., Flunkert, V., Gasthaus, J., and Januschowski, T. Deepar: Probabilistic forecasting with autoregressive recurrent networks. *International Journal of Forecasting*, 36(3):1181–1191, 2020.
- Seeger, M. W., Salinas, D., and Flunkert, V. Bayesian intermittent demand forecasting for large inventories. In *Advances in Neural Information Processing Systems*, pp. 4646–4654, 2016.
- Sen, R., Yu, H.-F., and Dhillon, I. Think globally, act locally: A deep neural network approach to high-dimensional time series forecasting. 2019.
- Tealab, A. Time series forecasting using artificial neural networks methodologies: A systematic review. *Future Computing and Informatics Journal*, 3(2):334–340, 2018.
- Vlahogianni, E. I., Karlaftis, M. G., and Golias, J. C. Short-term traffic forecasting: Where we are and where we’re going. *Transportation Research Part C: Emerging Technologies*, 43:3–19, 2014.
- Wang, Y., Smola, A., Maddix, D. C., Gasthaus, J., Foster, D., and Januschowski, T. Deep factors for forecasting. *arXiv preprint arXiv:1905.12417*, 2019.
- Wang, Z., Qinami, K., Karakozis, I. C., Genova, K., Nair, P., Hata, K., and Russakovsky, O. Towards fairness in visual recognition: Effective strategies for bias mitigation. In *Proceedings of the IEEE/CVF Conference on Computer Vision and Pattern Recognition*, pp. 8919–8928, 2020.
- Ward, R., Wu, X., and Bottou, L. Adagrad stepsizes: Sharp convergence over nonconvex landscapes. In *International Conference on Machine Learning*, pp. 6677–6686, 2019.
- Xu, L., Wang, S., and Tang, R. Probabilistic load forecasting for buildings considering weather forecasting uncertainty and uncertain peak load. *Applied Energy*, 237:180–195, 2019.
- Yu, T., Liu, X.-W., Dai, Y.-H., and Sun, J. A variable metric mini-batch proximal stochastic recursive gradient algorithm with diagonal barzilai-borwein stepsize. *arXiv preprint arXiv:2010.00817*, 2020.
- Zhang, G. P. Time series forecasting using a hybrid arima and neural network model. *Neurocomputing*, 50:159–175, 2003.
- Zhang, T. Solving large scale linear prediction problems using stochastic gradient descent algorithms. In *Proceedings of the twenty-first international conference on Machine learning*, pp. 116, 2004.

Zhou, P., Feng, J., Ma, C., Xiong, C., Hoi, S. C. H., et al.  
Towards theoretically understanding why sgd generalizes  
better than adam in deep learning. *Advances in Neural  
Information Processing Systems*, 33, 2020.

---

# Variance Reduction in Training Forecasting Models with Subgroup Sampling (Supplementary Materials)

---

## A. Details in Experiments and Additional Results

### A.1. Practical Version of SCott

We first discuss in details on the practical version of SCott as mentioned in Section 6. The full description is shown in Algorithm 2. The main difference between the plain SCott and Algorithm 2 is the latter treats the period  $K$  of performing subgroup sampling as a constant, while adaptively altering  $K$  based on a stopping criteria as highlighted in the blue text. Adopting such technique, despite being complicated in theory, allows us to adaptively perform the subgroup sampling based on the progress of the training. The hyperparameter  $\gamma$  can then be obtained via standard tuning algorithms such as grid search and random search.

---

**Algorithm 2** The practical version of SCott, where we apply the early stopping technique as shown in the blue text, instead of choosing  $K$  based on Geometric distribution.

---

**Require:** Total number of iterations  $T$ , learning rate  $\{\alpha_t\}_{1 \leq t \leq T}$ , initialize  $\theta^{(0,0)}$ , the set of groups:  $\{\mathcal{D}_i\}_{1 \leq i \leq B}$ , initialized selection of  $K$ , hyperparameter  $\gamma$ .

- 1: **for**  $t = 0, 1, \dots, T - 1$  **do**
  - 2:   Sample a  $\xi_i^{(t)}$  from subgroup  $i$  and perform subgroup sampling (with  $w_i = |\mathcal{D}_i|/|\mathcal{D}|$ ):  
 $\mathbf{g}^{(t,0)} = \sum_{i=1}^B w_i \nabla f_{\xi_i^{(t)}}(\theta^{(t,0)})$ .
  - 3:   **for**  $k = 0, 1, \dots, K - 1$  **do**
  - 4:     Sample  $\xi^{(t,k)}$  from  $\mathcal{D}$ .
  - 5:     Compute the update  $\mathbf{v}^{(t,k)}$  as  $\nabla f_{\xi^{(t,k)}}(\theta^{(t,k)}) - \nabla f_{\xi^{(t,k)}}(\theta^{(t,0)}) + \mathbf{g}^{(t,0)}$ .
  - 6:     Update the parameters as  $\theta^{(t,k+1)} = \theta^{(t,k)} - \alpha_t \mathbf{v}^{(t,k)}$ .
  - 7:     **if**  $\|\mathbf{v}^{(t,k)}\|^2 \leq \gamma \|\mathbf{v}^{(t,0)}\|^2$  **then**
  - 8:       **break**
  - 9:     **end if**
  - 10:   **end for**
  - 11:   Set  $\theta^{(t+1,0)} = \theta^{(t,k+1)}$ .
  - 12: **end for**
  - 13: **return** Sample  $\hat{\theta}^{(T)}$  from  $\{\theta^{(t,0)}\}_{t=0}^{T-1}$  with  $\mathbb{P}(\hat{\theta}^{(T)} = \theta^{(t,0)}) \propto \alpha_t B$
- 

### A.2. Synthetic Dataset Generation

In this subsection, we introduce the details of generating synthetic time series dataset as used in the experiments. We first set the context length to be 72 and prediction length to be 24. This synthetic dataset contains 4 time series with different patterns on their time horizon. We start from the definition of four types of patterns:  $\mathbf{t} = [1, 2, \dots, 23, 24] \in \mathbb{R}^{24}$ ,  $P_1 = \sin(\mathbf{t}) \in \mathbb{R}^{24}$ ,  $P_2 = \mathbf{t} \in \mathbb{R}^{24}$ ,  $P_3 = \mathbf{t}^2 \in \mathbb{R}^{24}$ ,  $P_4 = \sqrt{\mathbf{t}} \in \mathbb{R}^{24}$ , where all the transformations are element-wise, e.g.  $\sin(\mathbf{t}) = [\sin(1), \sin(2), \dots, \sin(23), \sin(24)]$ . And the four patterns are four different time series slices of length 24 that maps  $\mathbf{t}$  to different values via transformations of *sin*, *linear*, *quadratic*, *square root*, respectively. With these patterns, the time series data are then constructed via concatenating the patterns with different orders on the time horizon. Specifically,

$$\begin{aligned}
 TS_1 &= \underbrace{[P_1, P_2, P_3, P_4, \dots, P_1, P_2, P_3, P_4]}_{[P_1, P_2, P_3, P_4] \text{ repeats } 2K \text{ times}} + \mathcal{N}(0, \mathbf{1}), \quad \text{where } \mathcal{N}(0, \mathbf{1}) \in \mathbb{R}^{192K} \\
 TS_2 &= \underbrace{[P_4, P_3, P_2, P_1, \dots, P_4, P_3, P_2, P_1]}_{[P_4, P_3, P_2, P_1] \text{ repeats } 2K \text{ times}} + \mathcal{N}(0, \mathbf{1}), \quad \text{where } \mathcal{N}(0, \mathbf{1}) \in \mathbb{R}^{192K}
 \end{aligned}$$

$$\begin{aligned}
 TS_3 &= \underbrace{[P_1, P_3, P_2, P_4, \dots, P_1, P_3, P_2, P_4]}_{[P_1, P_3, P_2, P_4] \text{ repeats } 2K \text{ times}} + \mathcal{N}(0, \mathbf{1}), \quad \text{where } \mathcal{N}(0, \mathbf{1}) \in \mathbb{R}^{192K} \\
 TS_4 &= \underbrace{[P_4, P_2, P_3, P_1, \dots, P_4, P_2, P_3, P_1]}_{[P_4, P_2, P_3, P_1] \text{ repeats } 2K \text{ times}} + \mathcal{N}(0, \mathbf{1}), \quad \text{where } \mathcal{N}(0, \mathbf{1}) \in \mathbb{R}^{192K}
 \end{aligned}$$

where  $\mathcal{N}(0, \mathbf{1})$  denotes a random vector where each coordinate is sampled from a normal distribution. We can see each time series is repeating a distinct order of the four patterns, forming a temporal pattern, on its time horizon. We let such temporal pattern repeat 2K times on the time horizon of each time series. Finally, a Gaussian noise is added to each time series to capture randomness. After generating the time series, we then extract the training examples via a sliding window which slides 24 timestamps<sup>8</sup> between adjacent training examples. With a simple calculation, the total number of training examples in this dataset is 32K.

**Pre-grouping Strategy.** From the data generation process, we can see in each time series contains exactly four types of mapping: take  $TS_1$ , the type of mappings on its time horizon are  $\forall i = 1, 2, 3, 4$ ,

$$\text{Mapping } i: [P_{(i+1) \bmod 4}, P_{(i+2) \bmod 4}, P_{(i+3) \bmod 4}] \rightarrow P_i$$

Same conclusions can be drawn on other time series. And then we can pre-group all the training examples via a simple judgemental policy: the training examples that belonging to the same time series and having same pattern in their prediction range are clustered to the same subgroup. The total number of subgroups is then 16.

### A.3. Details of the Real-World Dataset Used.

- *Traffic*: A collection of hourly data from the California Department of Transportation. The data describes the road occupancy rates (between 0 and 1) measured by different sensors on San Francisco Bay area free ways. For this dataset, we set  $\tau_c = 3$  days (72 hours) and  $\tau_p = 1$  day (24 hours).
- *Exchange-Rate*: the collection of the daily exchange rates of eight foreign countries including Australia, British, Canada, Switzerland, China, Japan, New Zealand and Singapore ranging from 1990 to 2016. For this dataset, we set  $\tau_c = 8$  days and  $\tau_p = 1$  day.
- *Electricity*: The electricity consumption in kWh was recorded hourly from 2012 to 2014, for  $n = 321$  clients. We converted the data to reflect hourly consumption. For this dataset, we set  $\tau_c = 3$  days (72 hours) and  $\tau_p = 1$  day (24 hours).

### A.4. Additional Results

#### A.4.1. RESULTS ADDITIONAL TO THE MAIN PAPER SETTINGS

In the main paper, we show the convergence curves of training MLP on Traffic dataset and training NBEATS on Electricity dataset. Here, we provide the additional curves of training MLP on Electricity dataset.

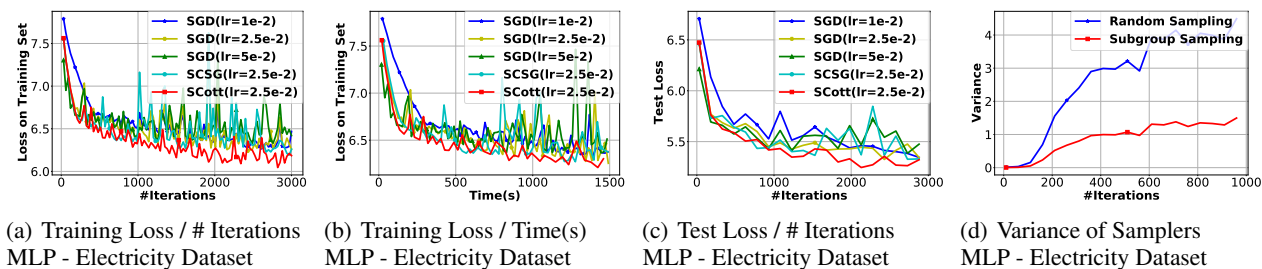


Figure 4. Additional Results of MLP on Electricity Dataset.

<sup>8</sup>We do this to guarantee each training example can include a completely different pattern in its prediction range. In practice, this can mean extracting training examples by day on a hourly measured time series.

**Algorithm 3** A Simple Grouping Algorithm Based on Long- and Short-Term Temporal Pattern

**Require:** original dataset  $\mathcal{D}$ , temporal patterns of different terms  $[\Delta_1, \dots, \Delta_m]$ .

- 1: Initialize the number of subgroups:  $B \leftarrow \frac{|\mathcal{D}| \prod_{j=2}^m \Delta_j}{\Delta_1}$
- 2: Initialized subgroups:  $\mathcal{D}_i \leftarrow \emptyset, \forall 1 \leq i \leq B$ .
- 3: **for**  $(i, t)$  in  $\mathcal{D}$  **do**
- 4:      $idx \leftarrow 0$
- 5:     **for**  $\Delta_j \in [\Delta_1, \dots, \Delta_m]$  **do**
- 6:          $idx \leftarrow idx + (t \bmod \Delta_j) \cdot \Delta_j$
- 7:     **end for**
- 8:      $\mathcal{D}_{idx+1} \leftarrow \mathcal{D}_{idx+1} \cup \{(i, t)\}$
- 9: **end for**
- 10: **return**  $\{\mathcal{D}_i\}_{i=1}^B$

## A.4.2. APPLYING EARLY STOPPING TECHNIQUE TO SCSG AND SVRG

In this subsection, we investigate how the baseline SCSG and SVRG would perform when the early stopping technique introduced in Section A.1 is applied on them. We rerun the MLP model on Traffic and Electricity dataset, and the fine tuned results are shown in Figure 5. In the literature, SVRG is shown to perform bad on deep learning tasks (Defazio & Bottou, 2018).

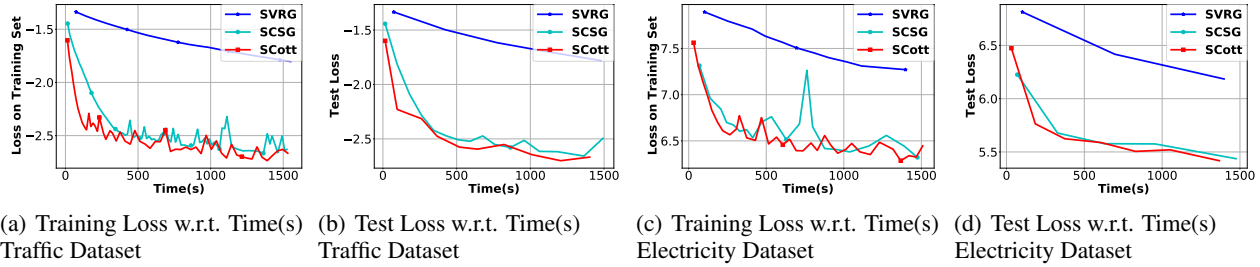


Figure 5. Applying the early stopping technique on SCSG and SVRG.

## A.5. Hyperparameter Tuning

We apply the grid search to tune the hyperparameters in each experiment, the grids for the step sizes are:  $\{0.1, 0.05, 0.025, 0.01, 0.005, 0.0025, 0.001, 0.0005, 0.00025, 0.0001\}$ . We set the weight decay to be  $1e-5$ . For experiments in Section 7.1 and 7.2, the optimal step size is specified. For SCott, we additionally tune  $\gamma$  from  $\{0.1, 0.125, 0.15, 0.2\}$ , and the optimal choice of  $\gamma$  on synthetic dataset is 0.125. Hyperparameters in other settings is shown in Table A.6. For the experiment in section 7.3, we have two extra hyperparameters  $\beta_1$  and  $\beta_2$ , we set the grids to be  $\{0.9, 0.99, 0.999\}$ . Finally, for  $\gamma$ , we extend the grids range to  $\{0.1, 0.125, 0.15, 0.2, 0.4, 0.8\}$ . The optimal choice of hyperparameter for each settings are shown in Table A.6.

## A.6. A Concrete example of pre-grouping with long- and short-term temporal pattern.

In the main paper, we discuss naively using the timestamp to pre-group the time series examples. Here we give a concrete pseudo code for such strategy, allowing pre-grouping with arbitrary long- and short-term temporal pattern (Lai et al., 2018).

Denote the temporal patterns available as  $\{\Delta_i\}_{i=1}^m$ . We know that each training example extracted is placed at a certain time point within each temporal interval, and we can use such information as features and apply a random hashing grouping on top of it. The detailed description for such algorithm is shown in Algorithm 3. Note that in the main paper, the pre-grouping strategy for *Traffic* and *Electricity* dataset can be seen as a special case of Algorithm 3 with two temporal intervals: weeks and seasons.

Table 4. Hyperparameters used for experiments on **real-world applications**. The format of the hyperparameters is shown as the following: the first value is the optimal choice of step size. For SCott-type optimizers, the last value is the optimal choice for  $\gamma$ . Additionally, the  $\beta_1$  and  $\beta_2$  for Adam-type optimizers are set to be 0.9 and 0.999 respectively for optimal performance.

| Model  | Dataset       | Optimizer |        |              |      |              |         |              |
|--------|---------------|-----------|--------|--------------|------|--------------|---------|--------------|
|        |               | SGD       | SCSG   | SCott        | Adam | S-Adam       | Adagrad | S-Adagrad    |
| MLP    | Exchange Rate | 5e-3      | 5e-2   | 5e-2/0.125   | 5e-3 | 5e-3/0.1     | 2.5e-2  | 2.5e-2/0.1   |
|        | Traffic       | 2.5e-2    | 2.5e-2 | 2.5e-2/0.125 | 5e-3 | 5e-3/0.125   | 5e-3    | 5e-3/0.125   |
|        | Electricity   | 2.5e-2    | 2.5e-2 | 2.5e-2/0.125 | 5e-3 | 2.5e-3/0.125 | 5e-3    | 2.5e-3/0.125 |
| NBEATS | Exchange Rate | 1e-3      | 1e-3   | 1e-3/0.1     | 1e-3 | 1e-3/0.1     | 1e-3    | 1e-3/0.1     |
|        | Traffic       | 1e-4      | 1e-4   | 2.5e-3/0.125 | 1e-4 | 1e-4/0.125   | 1e-4    | 1e-4/0.125   |
|        | Electricity   | 5e-3      | 1e-2   | 1e-2/0.125   | 1e-2 | 1e-2/0.125   | 1e-2    | 1e-2/0.125   |

## B. Proof to the lemmas and theorems.

### B.1. Proof to Lemma 1

*Proof.* Note that for AR(1), the model only has a single parameter. In this proof,  $\theta$  and  $[\theta]$  are interchangeable. The loss functions at different time can be expressed as:

$$f_{1,t}(\theta) = f_{1,t}([\theta]) = \begin{cases} (\delta\theta + 1 + \epsilon_t)^2 & t \bmod 4 = 0 \\ (\theta - \delta - \epsilon_t)^2 & t \bmod 4 = 1 \\ (\delta\theta + 1 - \epsilon_t)^2 & t \bmod 4 = 2 \\ (\theta - \delta + \epsilon_t)^2 & t \bmod 4 = 3 \end{cases},$$

Take gradient with respect to the model parameter  $\theta$  and without the loss of generality, taking  $\theta^{(0)} = [0]$ , we obtain

$$\nabla f_{1,t}([0]) = \begin{cases} 2\delta + 2\delta\epsilon_t & t \bmod 4 = 0 \\ -2\delta - 2\epsilon_t & t \bmod 4 = 1 \\ 2\delta - 2\delta\epsilon_t & t \bmod 4 = 2 \\ -2\delta + 2\epsilon_t & t \bmod 4 = 3 \end{cases}. \quad (14)$$

As defined by Equation (1), the gradient on the total loss can be expressed as (with out the loss of generality, we set  $T = 4\tilde{T}$  where  $\tilde{T}$  is an integer.)

$$\nabla f(\theta^{(0)}) = \frac{1}{T} \sum_{t=1}^T \nabla f_{1,t}(\theta^{(0)}) = \frac{2}{T} \sum_{m=0}^{\tilde{T}-1} (-\epsilon_{m+1} - \delta\epsilon_{m+2} + \epsilon_{m+3} + \delta\epsilon_{m+4}). \quad (15)$$

Denote  $\mathcal{E}$  as the event of "two training examples in the mini-batch are either both sampled from  $\mathcal{D}_1$  or both sampled from  $\mathcal{D}_2$ ". Depend on the event of  $\mathcal{E}$ , we first obtain when the event  $\mathcal{E}$  happens,

$$\mathbb{V} \left[ \nabla f_{\xi^{(0)}}(\theta^{(0)}) \middle| \mathcal{E} \right] \quad (16)$$

$$= \frac{1}{T^2} \sum_{t,t' \bmod 4=0} \left| 2\delta + \delta\epsilon_t + \delta\epsilon_{t'} - \frac{2}{T} \sum_{m=0}^{\tilde{T}-1} (-\epsilon_{m+1} - \delta\epsilon_{m+2} + \epsilon_{m+3} + \delta\epsilon_{m+4}) \right|^2 \quad (17)$$

$$+ \frac{1}{T^2} \sum_{t,t' \bmod 4=1} \left| -2\delta - \epsilon_t - \epsilon_{t'} - \frac{2}{T} \sum_{m=0}^{\tilde{T}-1} (-\epsilon_{m+1} - \delta\epsilon_{m+2} + \epsilon_{m+3} + \delta\epsilon_{m+4}) \right|^2 \quad (18)$$

$$+ \frac{1}{T^2} \sum_{t,t' \bmod 4=2} \left| 2\delta - \delta\epsilon_t - \delta\epsilon_{t'} - \frac{2}{T} \sum_{m=0}^{\tilde{T}-1} (-\epsilon_{m+1} - \delta\epsilon_{m+2} + \epsilon_{m+3} + \delta\epsilon_{m+4}) \right|^2 \quad (19)$$

$$+ \frac{1}{T^2} \sum_{t, t' \bmod 4=3} \left| -2\delta + \epsilon_t + \epsilon_{t'} - \frac{2}{T} \sum_{m=0}^{\tilde{T}-1} (-\epsilon_{m+1} - \delta\epsilon_{m+2} + \epsilon_{m+3} + \delta\epsilon_{m+4}) \right|^2 \quad (20)$$

$$+ \frac{1}{T^2} \sum_{t \bmod 4=0, t' \bmod 4=2} \left| 2\delta + \delta\epsilon_t - \delta\epsilon_{t'} - \frac{2}{T} \sum_{m=0}^{\tilde{T}-1} (-\epsilon_{m+1} - \delta\epsilon_{m+2} + \epsilon_{m+3} + \delta\epsilon_{m+4}) \right|^2 \quad (21)$$

$$+ \frac{1}{T^2} \sum_{t \bmod 4=2, t' \bmod 4=0} \left| 2\delta - \delta\epsilon_t + \delta\epsilon_{t'} - \frac{2}{T} \sum_{m=0}^{\tilde{T}-1} (-\epsilon_{m+1} - \delta\epsilon_{m+2} + \epsilon_{m+3} + \delta\epsilon_{m+4}) \right|^2 \quad (22)$$

$$+ \frac{1}{T^2} \sum_{t \bmod 4=1, t' \bmod 4=3} \left| -2\delta - \epsilon_t + \epsilon_{t'} - \frac{2}{T} \sum_{m=0}^{\tilde{T}-1} (-\epsilon_{m+1} - \delta\epsilon_{m+2} + \epsilon_{m+3} + \delta\epsilon_{m+4}) \right|^2 \quad (23)$$

$$+ \frac{1}{T^2} \sum_{t \bmod 4=3, t' \bmod 4=1} \left| -2\delta + \epsilon_t - \epsilon_{t'} - \frac{2}{T} \sum_{m=0}^{\tilde{T}-1} (-\epsilon_{m+1} - \delta\epsilon_{m+2} + \epsilon_{m+3} + \delta\epsilon_{m+4}) \right|^2 \quad (24)$$

$$\leq \frac{4}{T^2} \sum_{t, t' \bmod 4=0} \delta^2 + \frac{1}{T^2} \sum_{t, t' \bmod 4=0} \left| \delta\epsilon_t + \delta\epsilon_{t'} - \frac{2}{T} \sum_{m=0}^{\tilde{T}-1} (-\epsilon_{m+1} - \delta\epsilon_{m+2} + \epsilon_{m+3} + \delta\epsilon_{m+4}) \right|^2 \quad (25)$$

...

$$+ \frac{4}{T^2} \sum_{t \bmod 4=3, t' \bmod 4=1} \delta^2 + \frac{1}{T^2} \sum_{t \bmod 4=3, t' \bmod 4=1} \left| \epsilon_t - \epsilon_{t'} - \frac{2}{T} \sum_{m=0}^{\tilde{T}-1} (-\epsilon_{m+1} - \delta\epsilon_{m+2} + \epsilon_{m+3} + \delta\epsilon_{m+4}) \right|^2 \quad (27)$$

where in the last step we apply  $|a + b|^2 \leq 2a^2 + 2b^2, \forall a, b \in \mathbb{R}$ , and we break each term into two parts. The first part is independent of  $\epsilon_t$  and is only related to  $\delta^2$ , and the second term is the average of some sequence of  $\epsilon_t$ . Then  $\mathbb{V} \left[ \nabla f_{\xi^{(0)}}(\boldsymbol{\theta}^{(0)}) \middle| \mathcal{E} \right]$  can be upper bounded by the following form

$$\mathbb{V} \left[ \nabla f_{\xi^{(0)}}(\boldsymbol{\theta}^{(0)}) \middle| \mathcal{E} \right] \leq O(\delta^2) + \mathcal{T}_\epsilon, \quad (28)$$

where  $\mathcal{T}_\epsilon$  is the term containing all the  $\epsilon_t$ . Next we prove that  $\mathcal{T}_\epsilon$  is a small quantity  $o(\delta)$  with high probability. Note that here all the  $\epsilon_t$  are i.i.d. random variables, by applying the Hoeffding's inequality, which is for i.i.d random variables  $Z_1, \dots, Z_N$  following Gaussian white noise distribution,

$$\mathbb{P} \left( \left| \frac{1}{N} \sum_{m=1}^N Z_m \right| > t \right) \leq e^{-2Nt^2}, \quad (29)$$

applying this to  $\mathcal{T}_\epsilon$ , we obtain (we show the derivation on the first term, the others are similar), with probability  $1 - e^{-2To(\delta)^2}$ ,

$$\left| \delta\epsilon_t + \delta\epsilon_{t'} - \frac{2}{T} \sum_{m=0}^{\tilde{T}-1} (-\epsilon_{m+1} - \delta\epsilon_{m+2} + \epsilon_{m+3} + \delta\epsilon_{m+4}) \right|^2 \quad (30)$$

$$\leq \frac{1}{4} \left| \frac{1}{\tilde{T}} \sum_{m=0}^{\tilde{T}-1} (\epsilon_{m+1} - \epsilon_{m+3}) \right|^2 + \frac{1}{4} \left| \frac{\delta}{\tilde{T}} \sum_{m=0}^{\tilde{T}-1} (\epsilon_{m+2} - \epsilon_{m+4} + \epsilon_t + \epsilon_{t'}) \right|^2 \quad (31)$$

$$\leq o(\delta). \quad (32)$$

Apply this to every term, we obtain with high probability,

$$\mathcal{T}_\epsilon \leq o(\delta). \quad (33)$$



We can do the similar analysis on  $\mathbb{V} \left[ \nabla f_{\xi^{(0)}}(\boldsymbol{\theta}^{(0)}) \middle| -\mathcal{E} \right]$ , and obtain  $\mathbb{V} \left[ \nabla f_{\xi^{(0)}}(\boldsymbol{\theta}^{(0)}) \middle| -\mathcal{E} \right] \leq o(\delta)$ . Here we omit this part for brevity.  $\square$

## B.2. Proof to Theorem 1

*Proof.* Since this theorem states the existence of a dataset, the proof of is done by constructing this dataset, that implies the construction process allows us to choose  $\delta$  and  $N$  freely.

When  $p = 1$ , we let  $\mathcal{D}$  contains one single time series of length  $p + 1$  and  $\delta = 0$ . It is straightforward to see the variance is zero and the theorem holds since  $0 = \Omega(0)$ .

When  $p \geq 2$ , the  $\mathcal{D}$  we construct contains  $N = 2 \lfloor p/2 \rfloor$  different time series, and each time series is of length  $p + 1$ . Since here  $p \geq 2$ , we have  $N \geq 2$ . Since the model is predicting the same time here (it is predicting time  $p + 1$  given time 1 to  $p$ ), we let  $c = \epsilon_p$  denote a fixed value<sup>9</sup>. Without the loss of generality let  $2c \leq \delta$  such that  $\max_{i,t} |z_{i,t}| = \delta$ . Within the proof of this theorem, we let  $\bar{p} = \lfloor p/2 \rfloor$ ,  $\mathcal{D}$  is constructed as the following:

$$\text{Time Series } i: \begin{cases} \left[ \frac{\delta}{2}, \underbrace{0, \dots, 0}_{p-1}, \frac{\delta}{2} + c \right], i = 1 \\ \left[ \underbrace{0, \dots, 0}_{i-2}, \frac{\delta}{2}, -\frac{\delta}{2}, \underbrace{0, \dots, 0}_{p-i}, c \right], 2 \leq i \leq \bar{p} \\ \left[ \underbrace{0, \dots, 0}_{\bar{p}}, \underbrace{\frac{\delta}{2}, \dots, \frac{\delta}{2}}_{p-\bar{p}}, \frac{\delta}{2} + c \right], \bar{p} + 1 \leq i \leq 2\bar{p}, \end{cases}$$

Fit in the MSE loss we obtain:

$$\begin{aligned} f_1(\boldsymbol{\theta}) &= \left( \frac{\delta}{2} - \frac{\delta}{2} \boldsymbol{\theta}_1 \right)^2 \\ f_i(\boldsymbol{\theta}) &= \left( \frac{\delta}{2} \boldsymbol{\theta}_{i-1} - \frac{\delta}{2} \boldsymbol{\theta}_i \right)^2, \forall 2 \leq i \leq \bar{p} \\ f_i(\boldsymbol{\theta}) &= \left( \frac{\delta}{2} - \frac{\delta}{2} \boldsymbol{\theta}_{\bar{p}+1} - \dots - \frac{\delta}{2} \boldsymbol{\theta}_p \right)^2, \forall \bar{p} + 1 \leq i \leq 2\bar{p} \end{aligned}$$

where  $f_i$  denotes the loss incurred on the  $i$ -th time series. The total loss function can then be expressed as

$$f(\boldsymbol{\theta}) = \frac{1}{2\bar{p}} \sum_{i=1}^{2\bar{p}} f_i(\boldsymbol{\theta}) = \frac{1}{2\bar{p}} \sum_{i=1}^{\bar{p}} f_i(\boldsymbol{\theta}) + \frac{1}{2\bar{p}} \sum_{i=\bar{p}+1}^{2\bar{p}} f_i(\boldsymbol{\theta}) = g_1(\boldsymbol{\theta}) + g_2(\boldsymbol{\theta}) \quad (34)$$

note that when taking derivative of function  $f$  with respect to the  $\boldsymbol{\theta}$ , the first  $\bar{p}$  coordinates will only be affected by  $g_1(\boldsymbol{\theta})$ , i.e.,

$$\frac{\partial f}{\partial \boldsymbol{\theta}_i} = \frac{\partial g_1}{\partial \boldsymbol{\theta}_i}, \forall i \leq \bar{p} \quad (35)$$

then we obtain

$$\|\nabla f(\boldsymbol{\theta})\|^2 = \sum_{j=1}^p \left| \frac{\partial f}{\partial \boldsymbol{\theta}_j} \right|^2 \geq \sum_{j=1}^{\bar{p}} \left| \frac{\partial f}{\partial \boldsymbol{\theta}_j} \right|^2 = \sum_{j=1}^{\bar{p}} \left| \frac{\partial g_1}{\partial \boldsymbol{\theta}_j} \right|^2 = \|\nabla g_1(\boldsymbol{\theta})\|^2 \quad (36)$$

<sup>9</sup>the  $\epsilon_p$  can be obtained by generating the dataset using the same random seed as used in the model.

((Carmon et al., 2019) Lemma 1) shows that for every  $\boldsymbol{\theta}$  with  $\boldsymbol{\theta}_{\bar{p}} = 0$ ,

$$\|\nabla g_1(\boldsymbol{\theta})\| \geq \frac{\delta^2}{4\bar{p}^{\frac{5}{2}}} \quad (37)$$

as a result, we obtain for every  $\boldsymbol{\theta}$  with  $\boldsymbol{\theta}_{\bar{p}} = 0$

$$\|\nabla f(\boldsymbol{\theta})\| \geq \frac{\delta^2}{4\bar{p}^{\frac{5}{2}}} \quad (38)$$

Without the loss of generality we set<sup>10</sup>  $\boldsymbol{\theta}^{(0)} = \mathbf{0}$ . Now if we look at the expression of function  $g_1$ , if the model starts from  $\mathbf{0}$ , it follows a "zero-respecting" property:  $\boldsymbol{\theta}_j$  will remain zero if fewer than  $j$  number of gradients on  $g_1$  is computed (Carmon et al., 2019). Define a filtration  $\mathcal{F}^{(t)}$  at iteration  $t$  as the sigma field of all the previous events happened before iteration  $t$ . Let  $\tau_i$  denote the recent time where sample  $i$  is sampled for computing the stochastic gradient. And let  $N_t$  be a random variable, denoting the largest number where  $\tau_1$  to  $\tau_{N_t}$  is strictly increasing. Since each sample is uniformly sampled, we obtain

$$\mathbb{P}[N^{(t+1)} - N^{(t)} = 1 | \mathcal{F}^{(t)}] \leq \frac{1}{2\bar{p}} \leq \frac{1}{\bar{p}} \quad (39)$$

Let  $q^{(t)} = N^{(t+1)} - N^{(t)}$ , with Chernoff bound, we obtain

$$\mathbb{P}[N^{(t)} \geq \bar{p}] = \mathbb{P}[e^{\sum_{j=0}^{t-1} q^{(j)}} \geq e^{\bar{p}}] \leq e^{-\bar{p}} \mathbb{E}[e^{\sum_{j=0}^{t-1} q^{(j)}}] \quad (40)$$

For the expectation term we know that

$$\mathbb{E}[e^{\sum_{j=0}^{t-1} q^{(j)}}] = \mathbb{E}\left[\prod_{j=0}^{t-1} \mathbb{E}\left[e^{q^{(j)}} | \mathcal{F}^{(j)}\right]\right] \leq \left(1 - \frac{1}{\bar{p}} + \frac{e}{\bar{p}}\right)^t \leq e^{t(e-1)/\bar{p}} \quad (41)$$

Thus we know

$$\mathbb{P}[N^{(t)} \geq \bar{p}] \leq e^{\frac{(e-1)t}{\bar{p}} - \bar{p}} \leq \omega \quad (42)$$

for every  $t \leq \frac{\bar{p}^2 + \bar{p} \log(\omega)}{(e-1)}$ . Take  $\omega = \frac{1}{2}$ , for any  $0 < \epsilon < \frac{\delta^2}{8\bar{p}^{\frac{5}{2}}} \leq \frac{\delta^2}{8\bar{p}^{\frac{5}{2}}}$ , we obtain

$$\mathbb{E}\|\nabla f(\boldsymbol{\theta})\| = \mathbb{P}(N^{(t)} \geq \bar{p}) \left[\|\nabla f(\boldsymbol{\theta})\| | N^{(t)} \geq \bar{p}\right] + \mathbb{P}(N^{(t)} < \bar{p}) \left[\|\nabla f(\boldsymbol{\theta})\| | N^{(t)} < \bar{p}\right] \quad (43)$$

$$\geq \frac{1}{2} \|\nabla f(\boldsymbol{\theta})\| \quad (44)$$

$$> \frac{1}{2} \cdot 2\epsilon \quad (45)$$

$$= \epsilon \quad (46)$$

where we use Equation (38). The gradient is calculated as follows:

$$\begin{aligned} \nabla f_1(\mathbf{0}) &= \left[ -\frac{\delta^2}{2}, \underbrace{0, \dots, 0}_{p-1} \right] \\ \nabla f_i(\mathbf{0}) &= \left[ \underbrace{0, \dots, 0}_p, 0 \right], 2 \leq i \leq \bar{p} \\ \nabla f_i(\mathbf{0}) &= \left[ \underbrace{0, \dots, 0}_{\bar{p}}, \underbrace{-\frac{\delta^2}{2}, \dots, -\frac{\delta^2}{2}}_{p-\bar{p}} \right], \bar{p} + 1 \leq i \leq 2\bar{p} \end{aligned}$$

<sup>10</sup>If the initialization  $\boldsymbol{v} \neq \mathbf{0}$ , we just need to replace all the  $\boldsymbol{\theta}$  with  $\boldsymbol{\theta} - \boldsymbol{v}$  in the original functions and the proof will be the same.

$$\nabla f(\mathbf{0}) = \left[ -\frac{\delta^2}{4\bar{p}}, \underbrace{0, \dots, 0}_{\bar{p}-1}, -\frac{\delta^2}{4\bar{p}}, \dots, -\frac{\delta^2}{4\bar{p}} \right]$$

The sampling variance in the first iteration:

$$\mathbb{V} \left[ \nabla f_{\xi^{(0)}}(\boldsymbol{\theta}^{(0)}) \right] = \mathbb{E}_{i \sim [2\bar{p}]} \|\nabla f_i(\mathbf{0}) - \nabla f(\mathbf{0})\|^2 \quad (47)$$

$$= \frac{1}{2\bar{p}} \left[ \left( \frac{2\bar{p}-1}{4\bar{p}} \right)^2 \delta^4 + \frac{p-\bar{p}}{16\bar{p}^2} \delta^4 \right] + \frac{\bar{p}-1}{2\bar{p}} \left[ \frac{p-\bar{p}+1}{16\bar{p}^2} \delta^4 \right] + \frac{\bar{p}}{2\bar{p}} \left[ \frac{1}{16\bar{p}^2} \delta^4 + (p-\bar{p}) \left( \frac{2\bar{p}-1}{4\bar{p}} \right)^2 \delta^4 \right] \quad (48)$$

$$\leq \frac{3}{\bar{p}} \delta^4 + \bar{p} \delta^4 \quad (49)$$

$$\leq \bar{p}^2 \quad (50)$$

the last step holds when we let  $\delta^4 \leq \min\{\bar{p}^3/6, \bar{p}\}$ . Since for every  $t \leq \frac{\bar{p}^2 + \bar{p} \log(\omega)}{(e-1)}$ ,  $\mathbb{E} \|\nabla f(\boldsymbol{\theta})\| \geq \epsilon$ , the lower bound on the iterations (number of gradients to be computed)  $T_b$  is

$$T_b = \Omega(\bar{p}^2) \rightarrow T_b = \Omega \left( \mathbb{V} \left[ \nabla f_{\xi^{(0)}}(\boldsymbol{\theta}^{(0)}) \right] \right). \quad (51)$$

Furthermore,

$$\mathbb{V} \left[ \nabla f_{\xi^{(0)}}(\boldsymbol{\theta}^{(0)}) \right] = \frac{1}{2\bar{p}} \left[ \left( \frac{2\bar{p}-1}{4\bar{p}} \right)^2 \delta^4 + \frac{p-\bar{p}}{16\bar{p}^2} \delta^4 \right] + \frac{\bar{p}-1}{2\bar{p}} \left[ \frac{p-\bar{p}+1}{16\bar{p}^2} \delta^4 \right] + \frac{\bar{p}}{2\bar{p}} \left[ \frac{1}{16\bar{p}^2} \delta^4 + (p-\bar{p}) \left( \frac{2\bar{p}-1}{4\bar{p}} \right)^2 \delta^4 \right] \quad (52)$$

$$\geq \frac{p-\bar{p}}{2} \left( \frac{2\bar{p}-1}{4\bar{p}} \right)^2 \delta^4 \quad (53)$$

$$= \Omega(\delta^4 p) \quad (54)$$

and thus we complete the proof.  $\square$

### B.3. Proof to Theorem 2

#### B.3.1. MAIN PROOF

*Proof.* Take the expectation with respect to the sampling randomness in the inner loop for  $\mathbf{v}^{(t,k)}$ , we obtain

$$\mathbb{E}_{\xi^{(t,k)}} \left[ \mathbf{v}^{(t,k)} \right] = \mathbb{E}_{\xi^{(t,k)}} \left[ \nabla f(\boldsymbol{\theta}^{(t,k)}; \xi^{(t,k)}) - \nabla f(\boldsymbol{\theta}^{(t,0)}; \xi^{(t,k)}) + \mathbf{g}^{(t,0)} \right] = \nabla f(\boldsymbol{\theta}^{(t,k)}) + \underbrace{\mathbf{g}^{(t,0)} - \nabla f(\boldsymbol{\theta}^{(t,0)})}_{=\zeta_t} \quad (55)$$

Due to  $\zeta_t$ , the main step for SCott ( $\mathbf{v}^{(t,k)}$ ) is a biased estimation of the true gradient  $\nabla f(\boldsymbol{\theta}^{(t,k)})$ . The challenge of the proof is to handle such biasedness. The rest of our analysis largely follows the proof routine in SCSG-type methods (Babanezhad Harikandeh et al., 2015; Lei et al., 2017; Li & Li, 2018). We do not take credit for those analysis.

Li & Li (2018) proposes a nice framework of analyzing stochastic control variate type algorithm, where in their framework, the control variate  $\mathbf{g}^{(t,0)}$  is computed via a randomly sampled mini-batch. This, as we discussed in the paper, can be seen as a special case of random grouping. The main difference of SCott is in bounding  $\zeta_t$  since here the noise is not from the random sampling. For brevity, we summarize several lemmas from previous work. and focus on analyzing  $\zeta_t$  in the main proof.

We summarize the main results in Lemma 4. We encourage readers to refer to (Li & Li, 2018) for complete derivation for this part of results. From Lemma 4 we obtain when  $\alpha_t L = cB^{-\frac{2}{3}}$  (where  $c$  is a numerical constant),

$$\alpha_t B \left( 2 - \frac{2}{B} - 2\alpha_t L - \frac{1}{1 - \alpha_t^2 L^2 B - \alpha_t^3 L^3 B^2} \right) \mathbb{E} \|\nabla f(\boldsymbol{\theta}^{(t,0)})\|^2 \quad (56)$$

$$\leq 2\mathbb{E}(f(\boldsymbol{\theta}^{(t-1,0)}) - f(\boldsymbol{\theta}^{(t,0)})) + 2\alpha_t B \left(1 + \alpha_t L + \frac{1}{B}\right) \mathbb{E}\|\zeta_t\|^2, \quad (57)$$

given  $\alpha_t L = cB^{-\frac{2}{3}}$ , we obtain

$$1 - \alpha_t^2 L^2 B - \alpha_t^3 L^3 B^2 \geq 1 - B^{-\frac{1}{3}} c^2 - c^3, \quad (58)$$

put it back together with  $\alpha_t L = cB^{-\frac{2}{3}}$ , we get,

$$cB^{\frac{1}{3}} \left(2 - \frac{2}{B} - 2cB^{-\frac{2}{3}} - \frac{1}{1 - B^{-\frac{1}{3}} c^2 - c^3}\right) \mathbb{E}\|\nabla f(\boldsymbol{\theta}^{(t,0)})\|^2 \quad (59)$$

$$\leq 2L\mathbb{E}(f(\boldsymbol{\theta}^{(t-1,0)}) - f(\boldsymbol{\theta}^{(t,0)})) + 2cB^{\frac{1}{3}} \left(1 + cB^{-\frac{2}{3}} + B^{-1}\right) \mathbb{E}\|\zeta_t\|^2, \quad (60)$$

select  $c \leq \frac{1}{4}$  we can get,

$$2 - \frac{2}{B} - 2cB^{-\frac{2}{3}} - \frac{1}{1 - B^{-\frac{1}{3}} c^2 - c^3} \geq \frac{1}{4} \quad (61)$$

$$1 + cB^{-\frac{2}{3}} + B^{-1} \leq 1.35. \quad (62)$$

Fit in Lemma 5, we obtain

$$\mathbb{E}\|\nabla f(\boldsymbol{\theta}^{(t,0)})\|^2 \leq \frac{8L\mathbb{E}(f(\boldsymbol{\theta}^{(t-1,0)}) - f(\boldsymbol{\theta}^{(t,0)}))}{cB^{\frac{1}{3}}} + 11 \sum_{i=1}^B w_i^2 \sigma_i^2. \quad (63)$$

Telescoping from  $t = 0$  to  $T - 1$ , we obtain

$$\mathbb{E}\|\nabla f(\hat{\boldsymbol{\theta}}^{(T)})\|^2 \leq \frac{8(f(\mathbf{0}) - \inf_{\boldsymbol{\theta}} f(\boldsymbol{\theta}))L}{cB^{\frac{1}{3}}T} + 11 \sum_{i=1}^B w_i^2 \sigma_i^2 \quad (64)$$

$$= O\left(\frac{(f(\mathbf{0}) - \inf_{\boldsymbol{\theta}} f(\boldsymbol{\theta}))L}{B^{\frac{1}{3}}T} + \sum_{i=1}^B w_i^2 \sigma_i^2\right), \quad (65)$$

given our selection on the value of  $B$ ,

$$\sum_{i=1}^B w_i^2 \sigma_i^2 \leq O(\epsilon^2), \quad (66)$$

and then, with

$$T = O\left(\frac{(f(\mathbf{0}) - \inf_{\boldsymbol{\theta}} f(\boldsymbol{\theta}))L}{B^{\frac{1}{3}}\epsilon^2}\right), \quad (67)$$

we obtain

$$\mathbb{E}\|\nabla f(\hat{\boldsymbol{\theta}}^{(T)})\| \leq \sqrt{\mathbb{E}\|\nabla f(\hat{\boldsymbol{\theta}}^{(T)})\|^2} \quad (68)$$

$$= \sqrt{O\left(\frac{(f(\mathbf{0}) - \inf_{\boldsymbol{\theta}} f(\boldsymbol{\theta}))L}{B^{\frac{1}{3}}T} + \sum_{i=1}^B w_i^2 \sigma_i^2\right)} \quad (69)$$

$$\leq \epsilon. \quad (70)$$

Applying Lemma 3, the total number of stochastic gradient being computed can then be calculated as

$$\sum_{t=0}^{T-1} (B + \mathbb{E}[K_t]) = 2BT = O\left(\frac{\Delta LB^{\frac{2}{3}}}{\epsilon^2}\right), \quad (71)$$

when  $B = |\mathcal{D}|$ , then  $\sigma_{|\mathcal{D}|}^2 = 0$ , the total number of gradients to be computed is

$$O\left(\frac{\Delta L |\mathcal{D}|^{\frac{2}{3}}}{\epsilon^2}\right), \quad (72)$$

when  $B \neq |\mathcal{D}|$ , then put in

$$B = O\left(\frac{B \sum_{i=1}^B w_i^2 \sigma_i^2}{\epsilon^2}\right), \quad (73)$$

the total number of gradients to be computed is

$$O\left(\frac{\Delta L \left(B \sum_{i=1}^B w_i^2 \sigma_i^2\right)^{\frac{2}{3}}}{\epsilon^{\frac{10}{3}}}\right). \quad (74)$$

And thus we complete the proof.  $\square$

### B.3.2. TECHNICAL LEMMA

**Lemma 3.** ((Horváth et al., 2020), Lemma 1) Let  $N \sim \text{Geom}(\gamma)$ , for  $\gamma > 0$ . Then for any sequence  $D_0, D_1, \dots$  with  $\mathbb{E}|D_N| \leq \infty$ ,

$$\mathbb{E}(D_N - D_{N+1}) = \left(\frac{1}{\gamma} - 1\right) (D_0 - \mathbb{E}D_N). \quad (75)$$

**Lemma 4.** ((Li & Li, 2018), Proof to Theorem 3.1) when  $\alpha_t L = cB^{-\frac{2}{3}}$ ,

$$\alpha_t B \left(2 - \frac{2}{B} - 2\alpha_t L - \frac{1}{1 - \alpha_t^2 L^2 B - \alpha_t^3 L^3 B^2}\right) \mathbb{E}\|\nabla f(\boldsymbol{\theta}^{(t,0)})\|^2 \quad (76)$$

$$\leq 2\mathbb{E}(f(\boldsymbol{\theta}^{(t-1,0)}) - f(\boldsymbol{\theta}^{(t,0)})) + 2\alpha_t B \left(1 + \alpha_t L + \frac{1}{B}\right) \mathbb{E}\|\zeta_t\|^2. \quad (77)$$

*Proof.* The proof can be established straightforwardly by considering the constant batch size case in (Li & Li, 2018).  $\square$

**Lemma 5.**

$$\mathbb{E}\|\zeta_t\|^2 \leq \sum_{i=1}^B w_i^2 \sigma_i^2. \quad (78)$$

*Proof.*

$$\mathbb{E}\|\zeta_t\|^2 \quad (79)$$

$$= \mathbb{E}\|\mathbf{g}^{(t,0)} - \nabla f(\boldsymbol{\theta}^{(t,0)})\|^2 \quad (80)$$

$$= \mathbb{E}\left\|\sum_{i=1}^B \frac{|\mathcal{D}_i| \nabla f(\boldsymbol{\theta}^{(t,0)}; \xi_i^{(t)})}{|\mathcal{D}|} - \nabla f(\boldsymbol{\theta}^{(t,0)})\right\|^2 \quad (81)$$

$$= \mathbb{E}\left\|\sum_{i=1}^B \frac{|\mathcal{D}_i| \nabla f(\boldsymbol{\theta}^{(t,0)}; \xi_i^{(t)})}{|\mathcal{D}|} - \sum_{i=1}^B \frac{|\mathcal{D}_i|}{|\mathcal{D}|} \nabla f(\boldsymbol{\theta}^{(t,0)})\right\|^2 \quad (82)$$

$$= \sum_{i=1}^B w_i^2 \mathbb{E}\left\|\nabla f(\boldsymbol{\theta}^{(t,0)}; \xi_i^{(t)}) - \nabla f(\boldsymbol{\theta}^{(t,0)})\right\|^2 + \sum_{i \neq i'} \mathbb{E}\langle \nabla f(\boldsymbol{\theta}^{(t,0)}; \xi_i^{(t)}) - \nabla f(\boldsymbol{\theta}^{(t,0)}), \nabla f(\boldsymbol{\theta}^{(t,0)}; \xi_{i'}^{(t)}) - \nabla f(\boldsymbol{\theta}^{(t,0)}) \rangle \quad (83)$$

$$\leq \sum_{i=1}^B w_i^2 \sigma_i^2 \tag{84}$$

where in the final step, we use the property that  $\xi_i^{(t)}$  is independent of  $\xi_{i'}^{(t)}$ . □